

**DEVELOPMENT OF POLYAMIDEIMIDE BASED
NANOFILTRATION MEMBRANES FOR
SEPARATION OF DYES AND SALTS IN TEXTILE
WASTEWATER TREATMENT**

**A Thesis Submitted to
the Graduate School of Engineering and Sciences of
İzmir Institute of Technology
in Partial Fulfillment of the Requirements for the Degree of**

MASTER OF SCIENCE

in Chemical Engineering

**by
Ayşe METECAN**

**July 2019
İZMİR**

We approve the thesis of Ayşe METECAN

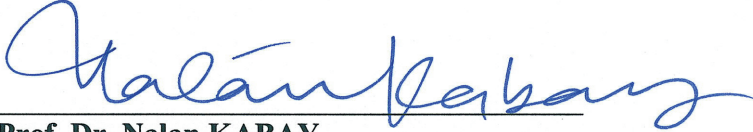
Examining Committee Members:



Prof. Dr. Sacide ALSOY ALTINKAYA
Department of Chemical Engineering, İzmir Institute of Technology



Prof. Dr. Erol ŞEKER
Department of Chemical Engineering, İzmir Institute of Technology



Prof. Dr. Nalan KABAY
Department of Chemical Engineering, Ege University

11 July 2019



Prof. Dr. Sacide ALSOY ALTINKAYA
Supervisor, Department of Chemical Engineering
İzmir Institute of Technology



Prof. Dr. Erol ŞEKER
Head of the Department of Chemical
Engineering

Prof. Dr. Aysun SOFUOĞLU
Dean of the Graduate School of
Engineering and Sciences

ACKNOWLEDGMENTS

Foremost, I would like to express my sincere gratitude to my advisor Prof. Dr. Sacide ALSOY ALTINKAYA for her support. I feel proud to have played a part in addressing global water issues under her supervision. Additionally, it has been a pleasure to learn from her about asking the right research questions and communicating clearly through academic publications and presentations.

I would like to also thank my committee members, Prof. Dr. Erol ŐEKER and Prof. Dr. Nalan KABAY for valuable suggestions to improve the quality of my thesis.

I am thankful to my co-worker Aydın CİHANOĐLU for his support, discussions, the sleepless nights when we were working together and for all the fun we have had. Without his help, I would never be able to finish my thesis. I thank my co-worker Elif GÜNGÖRMÜŐ DELİİSMAIL for her support, friendships, and assistance to my work.

I also would like to thank the Environmental Research Center, Biotechnology and Bioengineering Application Research Center, and Material Research Center at the İzmir Institute of Technology for their kind help and technical support.

I would like to thank Ekoten Fabrics for the real textile wastewater samples and analysis. Also, I would like to thank Dye Star for dye samples.

I also would like to thank my friends Gözde GÖZEL, Suna SOP, Esin GÖKMEN, Gizem CİHANOĐLU, and Azime ARIKAYA for their unconditional help, friendship, encouragement, and motivation.

The most lovely thanks, I would like to give to my husband, Ömer Engin METECAN for making my life meaningful and colorful. I fall short of words in expressing my gratitude towards him. Without his support, I would never be able to finish my thesis.

Above all, I am most grateful to my dear family members Berrin ÇOBAN, Yılmaz ÇOBAN and Bilge ÇOBAN for their eternal support, never-ending love, and encouragement during all my educational life. Also, I would like to thank FeriŐtah METECAN and İsmail Hakkı METECAN, my second family, for all their support and deepest love.

ABSTRACT

DEVELOPMENT OF POLYAMIDEIMIDE BASED NANOFILTRATION MEMBRANES FOR SEPARATION OF DYES AND SALTS IN TEXTILE WASTEWATER TREATMENT

The textile wastewater contains a significant level of organic dyes and inorganic salts. Separation of a vast amount of organic dyes and inorganic salts is important not only to comply with strict regulations but also to recover dyes for reuse during the process. Nanofiltration is proposed as a cost-effective alternative solution for dye and salt separation compared to traditional techniques. The main objective of this thesis is to develop a polyamideimide based positively charged nanofiltration membranes with high permeability, and high selectivity for separation of dyes and salts in textile wastewater treatment. Polyamide-imide (PAI) is an excellent choice for membrane production because of its superior processability, good mechanical features, and high chemical and thermal resistance. Its imide groups are crosslinked with polyethyleneimine (PEI), which is a suitable material to obtain a positively charged surface. In this study, support membranes of various pore sizes were produced by changing the composition of the coagulation bath and casting solution during the phase inversion method. Then, the optimum support membrane was in-situ modified with the alginate and coordinated with the metal ions for high permeability and high selectivity. The influences of the metal concentration and reaction time on the membrane performances were examined. It has been demonstrated that resulted nanofiltration membrane has high solute permeability ($>22 \text{ L} / \text{m}^2 \text{ h bar}$), high dye rejection ($\sim 95 \%$) and low salt rejection ($\sim 11 \%$). Moreover, this membrane was tested in the treatment of real textile wastewater samples. Salts in wastewater permeated, while high amounts of dye were rejected.

ÖZET

TEKSTİL ATIKSUYUNUN ARITIMINDA BOYA VE TUZLARIN AYRIŞTIRILMASI İÇİN POLAMİDİMİD BAZLI NANOFİLTRASYON MEMBRANLARININ GELİŞTİRİLMESİ

Tekstil atık suları önemli miktarda organik boya ve inorganik tuz içerir. Organik boya ve inorganik tuzun ayrılması, yalnızca yasal düzenlemelere uymak için değil, aynı zamanda işlem sırasında tekrar kullanılmak üzere boyaları geri kazanmak için de önemlidir. Nanofiltrasyon, geleneksel tekniklere kıyasla boya ve tuz ayırma için uygun maliyetli bir alternatif çözüm olarak önerilmiştir. Bu tezin temel amacı, tekstil atıksu arıtımında boya ve tuzların ayrılması için yüksek geçirgenliğe ve yüksek seçiciliğe sahip bir poliamid-imid (PAI) bazlı nanofiltrasyon membranı geliştirmektir. PAI, üstün işlenebilirlik, yüksek mekanik özelliği ile , yüksek kimyasal ve termal direnci nedeniyle membran üretimi için mükemmel bir seçimdir. İmid grupları, pozitif yüklü bir membran elde etmek için uygun bir malzeme olan polietilenimin (PEI) ile çapraz bağ yapabilir. Bu çalışmada, faz inversiyon yöntemi kullanılarak, koagülasyon banyosunun ve döküm çözeltisinin bileşiminin değiştirilmesi suretiyle çeşitli gözenek boyutlarında destek membranları üretilmiştir. Optimize edilen destek membranı aljinat ile modifiye edilmiş, ardından yüksek geçirgenlik ve yüksek seçicilik için metal iyonlarıyla koordine edilmiştir. Metal konsantrasyonunun ve reaksiyon süresinin membran performansına olan etkileri incelenmiştir. Elde edilen nanofiltrasyon membranının yüksek geçirgenliğe ($> 22 \text{ L /m}^2 \text{ h bar}$), yüksek boya reddine ($\sim \% 95$) ve düşük tuz reddine ($\sim \% 11$) sahip olduğu gösterilmiştir. Ayrıca, bu membran, gerçek tekstil atıksu numunelerinin arıtılmasında test edilmiştir. Sonuç olarak, tuzların membrandan geçtiği boya ve renkli bileşiklerin ise önemli oranda membran tarafından tutulduğu belirlenmiştir. Elde edilen membranlar Taramalı Elektron Mikroskobu (SEM), Enerji Dağılımlı X-Ray Analizi (EDX), Zeta Potansiyeli, Atomal Kuvvet Mikroskopisi ve Temas Açısı ölçümü ile karakterize edilmiştir.

TABLE OF CONTENTS

LIST OF FIGURES	viii
LIST OF TABLES	xii
CHAPTER 1. INTRODUCTION	1
CHAPTER 2. LITERATURE REVIEW	4
2.1. Membrane Separation Process	4
2.2. Nanofiltration	6
2.3. Properties of Textile Wastewater	9
2.4. Positively Charged NF membranes used for Textile Wastewater Treatment.....	9
2.4.1. Chemical or Thermal Treatment of the Support Membrane	11
2.4.2. Growth of a Layer on a Support	13
2.4.3. Surface Modification with Inorganic Compounds	15
CHAPTER 3. MATERIALS AND METHODS	20
3.1. Materials	20
3.2. Membrane Preparation.....	20
3.2.1. Preparation of Support Membranes by Phase Inversion Method	21
3.2.2. Surface Modification of Support Membrane.....	21
3.3. Filtration Experiment	23
3.3.1. Water Flux Measurement	23

3.3.2. Rejection Measurement	23
3.4. Characterization of the Membranes	25
3.4.1. Atomic Force Microscopy (AFM).....	25
3.4.2. Scanning Electron Microscopy (SEM).....	26
3.4.3. Contact Angle	26
3.4.4. Zeta Potential.....	26
3.4.5. Stability Test.....	27
3.4.6. Long Term Separation Performance.....	27
CHAPTER 4. RESULTS AND DISCUSSION.....	29
4.1. Preparation of Support Membranes by Phase Inversion Method	29
4.1.1. Effect of Coagulation Bath Composition	29
4.1.2. Effect of Polymer Concentration.....	32
4.2. Surface Modification of Prepared Membranes with Zinc Nitrate	33
4.3. Surface Modification of Prepared Membranes with Alginate	39
CHAPTER 5. CONCLUSIONS	54
REFERENCES	55

LIST OF FIGURES

<u>Figure</u>	<u>Page</u>
Figure 2.1. Schematic illustration of two-phase system separated via a membrane.	4
Figure 2.2. Illustration of pressure driven based membrane processes.	6
Figure 2.3. Schematic representation of phase inversion technique.	8
Figure 2.4. Ternary phase diagram of polymer, solvent and nonsolvent.	8
Figure 2.5. Wastewater of manufacturing industry by sectors 2016, Turkey.	10
Figure 2.6. Performance of the membrane as a function of pH (100 ppm dye, at 1 bar)....	14
Figure 2.7. The effect of PEI concentrations on the dye rejection and permeation flux of the fabricated membrane (GA concentration: 0.1 wt %, at 2 bar).	14
Figure 2.8. Influence of a) Tannic acid concentration and b) coating time on congo red permeability and rejection (Coating conditions: a) 2 g/L PEI and coating time of 10 min; b) 2 g/L PEI and 0.6 g/L TA).	15
Figure 2.9. The effect of a) the Co^{+2} concentration and b) the growth times of LDHs on membrane performance.	15
Figure 2.10. The pure water permeability and the salt rejection of the metal-functionalized nanofiltration membrane with different a) $\text{Zn}(\text{NO}_3)_2$ concentration and b) reaction time.	16
Figure 2.11. The flux and the organic/salt rejection of the metal-functionalized nanofiltration membrane.	17

<u>Figure</u>	<u>Page</u>
Figure 2.12. The influence of FeCl ₃ concentration on the separation performance of the membrane.....	18
Figure 2.13. Long-term separation performance of the resulting membrane for a) model solution and b) real textile wastewater.....	18
Figure 2.14. The effect of reaction time on dye rejection and pure water flux of the nanofiltration membranes (at 2 bar).....	19
Figure 3.1. Structure of polymers (a) PAI (b) PEI (c) ALG.....	22
Figure 3.2. Alginate deposition under dynamic condition.....	22
Figure 3.3. Dead-End Unit.....	24
Figure 3.4. Crossflow filtration unit.	28
Figure 4.1. The crosslinking reaction between PAI and PEI.....	30
Figure 4.2. The effect of PEI concentration on a) the pure water permeability (PWP) and b) dye and salt rejection (pH3).....	31
Figure 4.3. The effect of PAI concentration on the pure water permeability.	32
Figure 4.4. The illustration of the coordination mechanism between PEI and Zn ²⁺	33
Figure 4.5. Effect of reaction time on dye rejection and permeability performances of membrane A.	34
Figure 4.6. Effect of Zn ²⁺ concentration on dye rejection and permeability performances of membrane A.....	35
Figure 4.7. Effect of reaction time on dye rejection and permeability performances of membrane D.	36

<u>Figure</u>	<u>Page</u>
Figure 4.8. Effect of reaction time on permeability and dye rejection performances of membrane E.	37
Figure 4.9. Effect of Zn ²⁺ concentration on dye rejection and permeability performances of membrane E.	38
Figure 4.10. Methylene Blue rejection performance of PAI/PEI membrane (bare) and PAI/PEI-Zn ²⁺ (modified) membrane.	39
Figure 4.11. Reaction mechanism between PEI and Alginate.....	40
Figure 4.12. Reaction mechanism between a) zinc or b) iron cations with alginate.	41
Figure 4.13. Effect of different metal ions on dye rejection and salt rejection performance (reaction time: 20 min, metal concentration: 10 mM).	42
Figure 4.14. Effect of different metal ions on dye rejection and salt rejection performance (reaction time: 120 min-metal ion concentration: 50mM).	43
Figure 4.15. Zeta potential as a function of pH for bare membrane (PAI/PEI), modified membrane (PAI/PEI/Alginate/Fe ³⁺).	44
Figure 4.16. Surface SEM images of the bare membrane (PAI/PEI) with magnification 10000x.	44
Figure 4.17. Surface SEM images of the modified membrane (PAI/PEI/Alginate/Fe ³⁺) with magnification 10000x.	45
Figure 4.18. Permeability of the bare membrane (PAI/PEI), alginate deposited membrane (PAI/PEI/Alginate) and, resulted membrane (PAI/PEI/Alginate/ Fe ³⁺).....	46
Figure 4.19. Water contact angle of bare membrane (PAI/PEI), alginate deposited membrane (PAI/PEI/Alginate) and, resulted membrane (PAI/PEI/Alginate/ Fe ³⁺).....	46

<u>Figure</u>	<u>Page</u>
Figure 4.20. AFM images of support membrane (PAI/PEI).....	47
Figure 4.21. AFM images of modified membrane (PAI/PEI_Alginate).	47
Figure 4.22. AFM images of modified membrane (PAI/PEI/Alginate/Fe ³⁺).	48
Figure 4.23. Long term separation performance of the membrane toward NaCl and methyl green.....	49
Figure 4.24. Fouling resistances and flux recovery ratio of the modified membrane after filtration of model solution for 72 h.	49
Figure 4.25. Throughput comparison of different membranes from literature.....	51
Figure 4.26. Long term separation performance of the resulted membrane toward real textile wastewater.....	52

LIST OF TABLES

<u>Table</u>	<u>Page</u>
Table 2.1. Membrane separation processes and corresponding driving forces and their applications.	5
Table 2.2. Applications of NF membranes.	7
Table 2.3. The discharge standards of textile wastewater.	10
Table 2.4. Main properties of real textile wastewater studied by several researchers. ..	11
Table 3.1. Devices for measurement of real textile wastewater parameters.	28
Table 4.1. Casting conditions for the support membranes.	30
Table 4.2. Casting conditions for the support membranes.	32
Table 4.3. Surface modification conditions with $Zn(NO_3)_2$	34
Table 4.4. Surface modification conditions with $Zn(NO_3)_2$	35
Table 4.5. Surface modification conditions with $Zn(NO_3)_2$	36
Table 4.6. Surface modification conditions with $Zn(NO_3)_2$	37
Table 4.7. Surface modification conditions with $Zn(NO_3)_2$	38
Table 4.8. Reaction Condition of Membrane E	42
Table 4.9. Reaction Condition of Membrane E	42

<u>Table</u>	<u>Page</u>
Table 4.10. EDX analysis of the bare (PAI/PEI) and modified (PAI/PEI/Alginate/Fe ³⁺) membranes.	43
Table 4.11. Surface roughness values of bare and modified membranes.	48
Table 4.12. Long-Term separation performance of various lab-scale NF membranes for dye desalination (Feed: 1000 ppm NaCl and 100 ppm dye or *500 ppm dye).	50
Table 4.13. Real textile wastewater properties.	53
Table 4.14. Membrane rejection performance in the treatment of real textile wastewater samples.	53

CHAPTER 1

INTRODUCTION

As is known, water is an indispensable necessity for the continuity of life. Although the amount of available water on our planet is very high, unfortunately, the freshwater resources are low. The clean water demand increases with population growth. Nowadays, more than 10 % of the world's population cannot reach clean water (Schwab 2016). The World Health Forum and the World Economic Forum identify this growing world water scarcity as a foremost crisis. To meet the need for freshwater, treatment of industrial wastewater, seawater, and brackish water is a direct solution. Therefore, this concern has forced mankind to discover efficient and sustainable technologies for water treatment. Adsorption, coagulation, oxidation and biological degradation are some of the most well-known techniques used for water purification. These methods are particularly insufficient for sustainable purifications to recover valuable components because of the degradation of the compound separated from water. It is a known fact that the membrane process is an environmentally friendly, cost-effective and sustainable technology that contributes greatly to the treatment of wastewater. The wastewater generated in the textile industry is highly polluted compared to the discharge in other industries. It contains a significant level of organic dyes and inorganic salts. Dyes are highly toxic, mutagenic and carcinogenic pollutant that affects the environment by polluting the freshwater or reducing light penetration and photosynthetic activity (Jun et al. 2019). For this reason, separation of a vast amount of organic dyes and inorganic salts are important not only to comply with strict regulations but also to recover dyes for reuse during the process. In addition, low salt rejection, when associated with the removal of dyes, can also ensure that wastewater is reused for washing cycles (Bengani-Lutz et al. 2017). In general, the molecular weight of dyes used in the textile industry ranges from 200 Da to 1000 Da (Li et al. 2019). UF membranes are insufficient in rejecting dyes due to their small molecular size. The nanofiltration membrane is suitable for dye rejection because it has a molecular weight cutoff (MWCO) of about 200-1000 Da corresponding to pore sizes of 0.5 to 2 nm

in diameter (Ismail and Jye 2017). In addition, NF membranes usually carry an electrostatic charge. Therefore, they may reject molecules smaller than their pore size.

Most NF membranes are negatively charged and they have a low isoelectric point which limit their application to reject cationic dyes, in addition, they suffer from fouling. As a kind of cationic polymer containing amine groups, polyethyleneimine (PEI) is commonly used to obtain positively charged surface or functional layer (Zhao and Wang 2017). Xu et al. (2016) co-deposited catechol and PEI onto polyacrylonitrile (PAN) UF substrate. While the bare membrane surface was negatively charged (-60 mV, at pH 7), the zeta potential of the coated membrane increased to 50 mV (Xu et al. 2016). Sun et al. (2012) formed hyperbranched polyethylenimine (PEI) layer on the polyamide-imide (PAI) hollow fiber membrane through interfacial polymerization. They reported nearly 100% rejection of Safranin O (350 Da), 85.5 % rejection of NaCl and 4.9 L/m² h bar of pure water permeability (Sun et al. 2012). Zhao et al. (2017) coated PEI and gallic acid (GA) on to the PAN UF substrate and the resulting membrane was exposed to thermal treatment. They demonstrated a high selectivity for dye (97,3 %) and salt (5 %) mixture (Zhao and Wang 2017). Han et al. (2018) produced loose NF hollow fiber membranes with a phase inversion method, then modified with PEI to make the membrane surface more hydrophilic and positively charged. While the permeation flux was approximately 15.8 L / m² h (at 1 bar), AB-8 (1299 Da) dye rejection and salt (Na₂SO₄) rejection were 99 % and 5 %, respectively, during 200 hours of filtration. This indicates the stability of hollow fibers for the dye/salt mixture filtration (Han et al. 2018). The polyethylenimine (PEI) has a chelating tendency to metal ions due to the pair of electrons which is unshared in the nitrogen atom (Ruey-Shin and Ming-Nan 1996). Zhao et al. (2018) used this ability of the PEI to produce layered double hydroxides structure which provides more transport channels and stability to the membrane. They achieved good separation performance and high permeability (Zhao et al. 2018). Yang et al. (2017) used the chelating tendency of PEI which allows growth of the ZIF-8 particle on the surface to overcome the tradeoff between permeability and selectivity in the literature. The positively charged NF membrane generated via coating of the PEI-copper(II) complex layer on the commercial PAN ultrafiltration membrane was then cross-linked with glutaraldehyde (GA). The salt rejection for the developed membrane was reported as 43.5 % while its flux was 3.23 L / m² h bar (Xu et al. 2015). A loose nanofiltration membrane was produced with a coordinated cross-linked Fe (III)-phos-(PEI) layer on the commercial PAN substrate. It

was reported that the obtained membrane has good dye-salt separation and the membrane flux of $5 \text{ L} / \text{m}^2 \text{ h bar}$ (Li, Wang, et al. 2018).

The main objective of this thesis is to develop a positively charged nanofiltration membrane with both high flux and high selectivity for the separation of dyes and salts in textile wastewater. In this approach, the polyethylenimine was dissolved in a coagulation bath to form chemical crosslinking with the polyamide-imide (PAI), then the resulting membrane was in-situ modified with the alginate and coordinated with the metal ions. The modified and unmodified membranes were characterized by Scanning Electron Microscopy (SEM), Energy dispersive X-Ray Analysis (EDX), Zeta Potential, Atomic Force Microscopy and Contact angle measurements.

In this thesis, there are 5 chapters including the Introduction section as Chapter 1. Brief information about membrane separation process, nanofiltration membrane, textile wastewater properties and recent studies on positively charged nanofiltration membranes for textile wastewater treatment are summarized in Chapter 2.

In Chapter 3, materials and methods used in membrane development, characterization, filtration and separation methods are explained. The results were presented and discussed in Chapter 4, Chapter 5 summarized the general conclusions obtained from this study.

CHAPTER 2

LITERATURE REVIEW

2.1. Membrane Separation Process

Membranes are defined as a selective barrier that permits the separation of two phases and restricts passage of several compounds in a very specific way (Porter 1991). Schematic illustration of the two-phase system separated via a membrane is indicated in Figure 2.1.

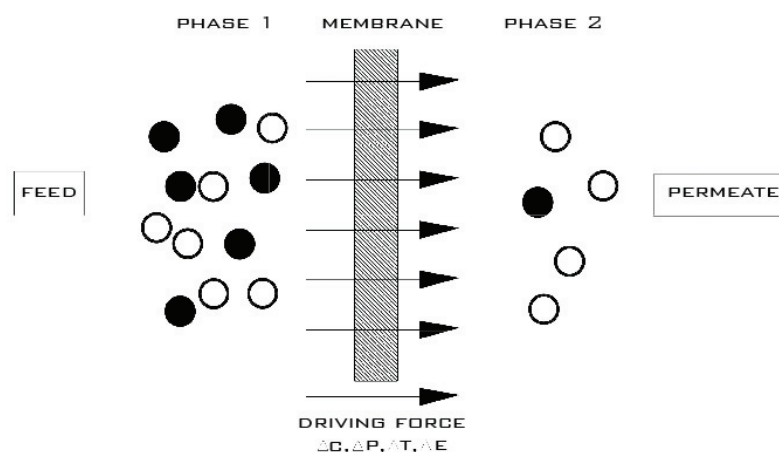


Figure 2.1. Schematic illustration of two-phase system separated via a membrane.
(Source: Adapted from Mulder 1997)

Phase 1 usually called the upstream side or feed phase which will be separated, while phase 2 is called the downstream side or permeate which passing through the membrane. Selective transport of one component compared to others depends on kinetic and thermodynamic factors. Typical driving forces applied in membrane separation processes are electrical potential difference, concentration or chemical potential difference, temperature difference and hydrostatic pressure difference. On the basis of the

main driving force applied, many membrane processes can be distinguished (Mulder 1997) and they are listed in Table 2.1 below.

Table 2.1. Membrane separation processes and corresponding driving forces and their applications. (Source: Adapted from Strathmann et al. 2006)

Driving Force	Membrane Process	Applications
Pressure difference	Microfiltration (MF)	Water purification and sterilization,
	Ultrafiltration (UF)	Recovery of macromolecules,
	Nanofiltration (NF)	Recovery of low molecular weight compounds,
	Reverse osmosis (RO)	Sea & breakish water desalination.
Chemical potential difference	Pervaporation (PV)	Separation of azeotropic mixtures,
	Dialysis (D)	Artificial kidney,
	Gas separation	Separation of gases and isotopes.
Electrical potential difference	Electrodialysis (ED)	Water desalination.
Temperature difference	Membrane Distillation (MD)	Water desalination, concentration of solutions.

Pressure driven membrane separation processes can be classified as microfiltration (MF), ultrafiltration (UF), nanofiltration (NF) and reverse osmosis (RO) in descending order with respect to the pore size (Figure 2.2).

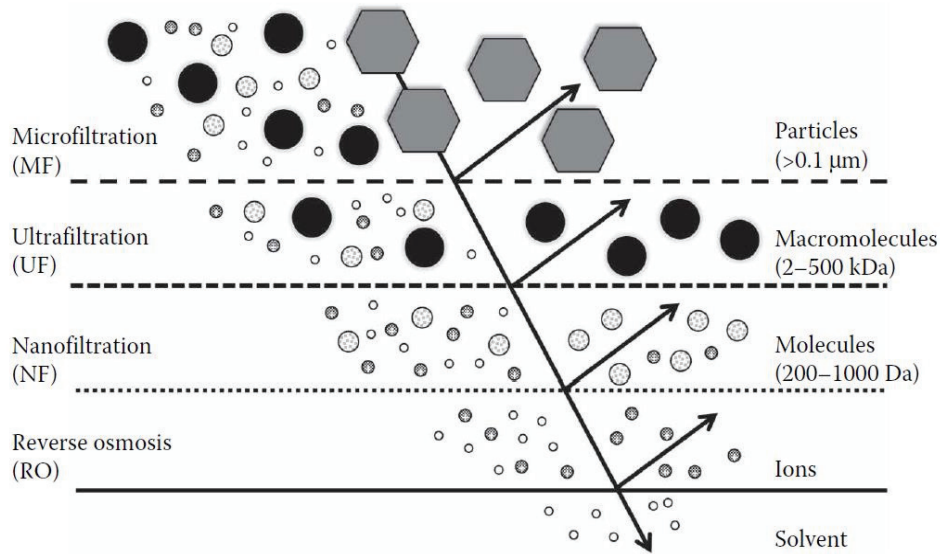


Figure 2.2. Illustration of pressure driven based membrane processes.
(Source: Taken from Ismail and Jye 2017)

2.2. Nanofiltration

Nanofiltration (NF) is the state of the art technology that was developed after microfiltration (MF), ultrafiltration (UF), and reverse osmosis (RO). In the 1970s, NF term is called as loose RO or tight UF. In the mid-1980s, FilmTech Company was first described NF membrane having features between RO and UF membranes. NF membrane has a molecular weight cutoff (MWCO) of about 200–1000 Dalton (Da), which corresponds to a pore size within the range of 0.5 and 2 nm in diameter (Fan et al. 2015). The separation by an NF membrane is achieved through a combination of both size exclusion and Donnan exclusion (Priyadarshini et al. 2018). The NF processes have applications in water treatment, wastewater treatment, food & dairy, pharmaceutical & biomedical, oil & gas industries (Table 2.2). The main advantages of NF processes can be listed as operational simplicity, specific component selectivity, low energy requirement, and environmental compatibility.

Donnan exclusion and size exclusion give an explanation of the separation mechanism for the NF membrane. The uncharged solute is carried by convection and diffusion depending on the pressure gradient and concentration gradient, respectively (Van der Bruggen et al. 1998). A sieving mechanism plays an important role in the

retention of uncharged solutes. In the case of charged molecules, an electrostatic interaction occurs between the molecules and the charged membrane, therefore, NF membranes may reject molecules that are smaller than their pore size. Changing the physical chemistry of the aqueous medium may result in optimum conditions for the charge interaction between the particles and membranes (Tu 2013). The NF membrane shows particularly high rejection at a pH far from the isoelectric point because the Donnan exclusion is most effective at these pH values.

Table 2.2. Applications of NF membranes. (Source: Taken from Ismail and Jye 2017)

Sector	Applications
Water treatment	water softening, color removal, micropollutants removal, pretreatment in RO process,
Wastewater treatment	leachate wastewater, textile effluent, emerging contaminants (ECs) removal, effluent from pulp and paper process
Food and dairy	whey protein desalination, caustic and acid recovery, gelation concentration
Pharmaceutical and biomedical	whey pre-concentration, whey protein desalination, gelation concentration, fractionation of proteins, plasma purification, filtration of DNA, RNA, and endotoxins, preparation of desalted and concentrated antibiotics, recovery of 6-amino penicillanic acid from waste stream
Oil and gas	solvent recovery from lube oil and hydrocarbon solvent mixtures, removal of sulfate from seawater before offshore reservoir injection

Most commercially available or laboratory sized NF membranes are usually produced by the phase inversion method as shown in Figure 2.3. In this process, first, the polymer is dissolved in a proper solvent, next, the polymer solution is spread on a nonwoven fabric or glass plate and immersed in a non-solvent coagulation bath. The homogeneous solution in the coagulation bath phase separates into polymer-lean and

polymer-rich phases. A ternary-phase diagram is used to understand the thermodynamics of membrane formation as shown in Figure 2.4. While the corners of the triangle symbolize three components (polymer, solvent, and non-solvent), any point outside the binodal line represents a homogeneous mixture. During coagulation of casting solution, solvent and nonsolvent exchange occurs. Once the polymer solution enters into the binodal line, polymer solution is no longer homogeneous and separates into phases. Precipitation rate controls the structure of the membrane. While slow precipitation rate produces sponge-like pores, fast precipitation results in finger-like pores (Guillen et al. 2011). By adjusting the properties of casting and coagulation bath conditions through changing the solvent type, polymer concentration, casting thickness, incorporating additives coagulation bath composition, and temperature, membranes with wide range of sizes can be obtained (Mulder 1997).

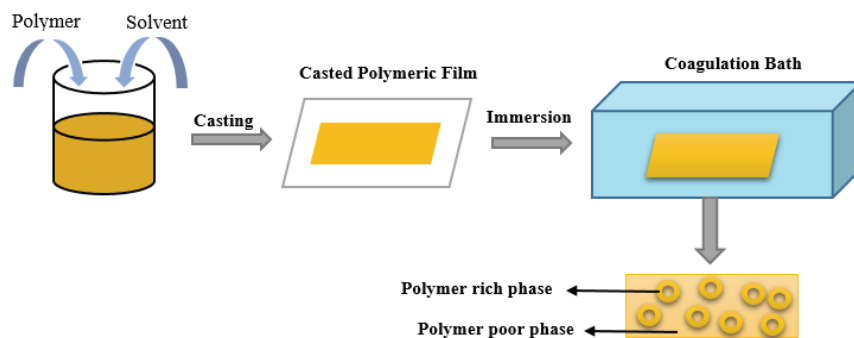


Figure 2.3. Schematic representation of phase inversion technique.

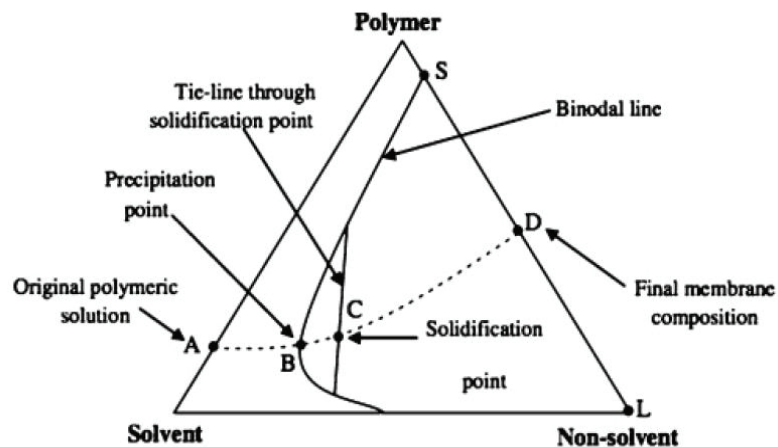


Figure 2.4. Ternary phase diagram of polymer, solvent and nonsolvent. (Source: Reprinted with permission from Jamil et al. 2015)

2.3. Properties of Textile Wastewater

The textile industry is one of the largest water consumer industry. Wastewater in the textile industry is generated during pre-treatment, dyeing, printing, and finishing steps. According to the Turkey Statistical Institute data, discharged wastewater from the textile industry is among the most pollutants of all the industries in Turkey (Figure 2.5). Textile wastewater contains surfactants, oil residues, complexing agents and especially a significant amount of organic dyes and inorganic salts (Bengani-Lutz et al. 2017). The composition and real textile wastewater properties have been compiled by Verma et al. (2012) as given in Table 2.4. During the dyeing process, not all dyes can be attached to the fabric. Therefore, these unattached dyes increase the contamination of textile wastewater. Approximately 200,000 tons of dyes are lost every year due to this inefficient dyeing process (Cheng et al. 2011). Dyes are highly toxic, mutagenic and carcinogenic substances that affect the environment through reducing light penetration and photosynthetic activity (Jun et al. 2019). The biggest challenge is to eliminate the color of wastewater. Furthermore, the textile wastewater contains volatile organic compounds (Verma, Dash, and Bhunia 2012). Therefore, there is still a need for an efficient treatment process in order to satisfy the discharge standard of textile wastewater (Table 2.3).

2.4. Positively Charged NF membranes used for Textile Wastewater Treatment

NF membranes prepared from polysulfone (PSf), poly(ether sulfone) (PES), poly(vinylidene fluoride) (PVDF), cellulose acetate (CA), polypropylene (PP), poly(acrylonitrile) (PAN), and polyamides membranes are either neutral or negatively charged in aqueous media (Peydayesh, Mohammadi, and Bakhtiari 2018). In general, these polymeric materials are amphoteric in nature and exhibit positively charged behavior only at low pHs Choundhury et al. (2018). This fact restricts the number of studies on the production of positively charged NF membranes and their application in the wide pH range in the textile industry. According to the Donnan exclusion mechanism,

the positively charged NF membranes exhibit excellent rejection for multivalent cations and cationic dyes. Negatively charged NF membranes suffer from poor rejection and high fouling tendencies when separating especially cationic molecules. In addition, commonly used polymers have reached the boundary between permeability and selectivity, they no longer meet the desired values. Therefore, “chemical or thermal treatment of the support membrane” or “growth of a layer on a support membrane” or “surface modification of the membrane with inorganic compound” are commonly used approaches to improve the properties of the membranes. Choundhury et al. (2018) reported that the number of publications related to the support membrane modification has increased fivefold since 2010. The surface modification of the membranes generally aims to form super hydrophilic and antibacterial surface layers, reduce surface roughness or increase the electrostatic surface charge (Choudhury et al. 2018). In the following section, methods used for modifying the support membranes are discussed.

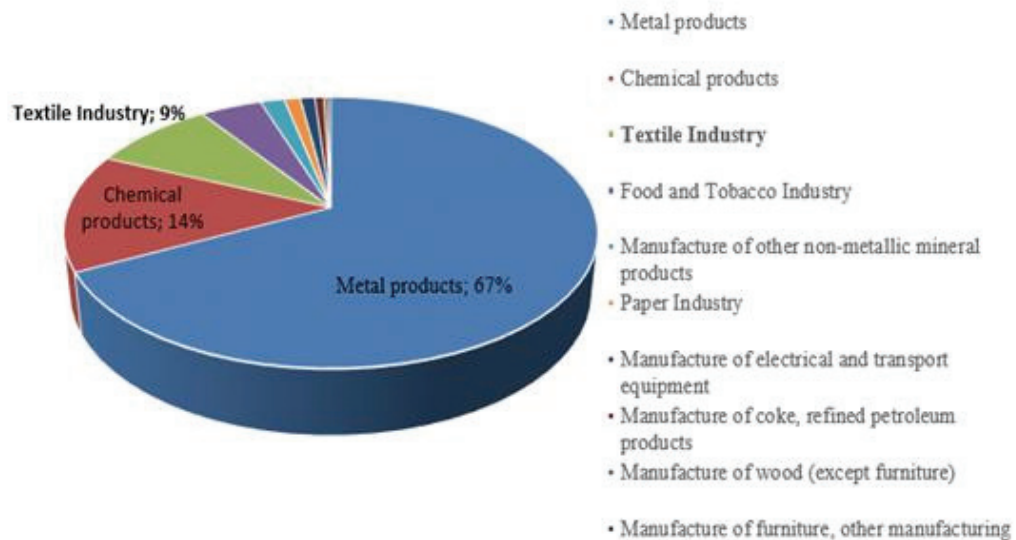


Figure 2.5. Wastewater of manufacturing industry by sectors 2016, Turkey. (Source: Turkish Statistical Institute 2016)

Table 2.3. The discharge standards of textile wastewater. (Source: Taken from Turkey-Ministry-of-Environment 2004)

Parameters	Discharge Standards
Chemical Oxygen Demand (COD) (mg/L)	250-400
Total Suspended Solids (TSS) (mg/L)	100-400
pH	6-9
Color (Pt-Co)	260-280

Table 2.4. Main properties of real textile wastewater studied by several researchers.
(Surce: Taken from Verma, Dash, and Bhunia 2012)

pH	COD (mg/L)	TSS (mg/ L)	TDS (mg/L)	Colour
8.8-9.4	595	276.00	-	-
11.2	2276	-	47.9	-
5-10	1100-4600	-	50	1450-1475
6.5-8.5	550-1000	100-400	-	7.5-25.5 ^b
2.7	7000	440	930	-
13.56	2968	-	-	3586 (C.U)
12-14	1500-2000	-	-	Dark Blue
10	1150	150	-	1.24 ^{436nm}
9	750	-	-	-
2-10	50-5000	50-500	-	>300(C.U)
8.32-9.5	278-736	85-354	1717-6106	-
8.7	17900	23900	1200	-
9.3	3900	-	-	-
7.8	810	64	-	0.15 ^{669nm}
13	2300	300	-	-
6.95	3422	1112	-	-
7.86	340	300	-	> 200 (Pt-Co)
7.5	131	75	1885	-

2.4.1. Chemical or Thermal Treatment of the Support Membrane

Ong et al. (2014) fabricated polyamide-imide membranes via the dry-jet wet-spinning method. The membrane was thermally treated with polyethyleneimine (60 kg/mol) at 70 °C to make the resulting support membrane hydrophilic and positively

charged. Negatively charged dyes such as reactive blue 19 (627 Da), reactive black 5 (992 Da) and reactive yellow 81 (1631 Da) were used to observe the effect of feed pH on the membrane separation performance. They demonstrated that the pH of the feed influenced the surface charge density and the permeate flux of the membrane, thereby significantly altered the dye rejection. The membrane exhibited high positive charge at acidic media (pH=3) due to protonation of amine groups in the polyethyleneimine and was fouled by the adsorption of the negatively charged dyes, as a result, permeate flux declined dramatically as portrayed in Figure 2.5. The membrane became negatively charged in the alkaline environment (pH = 10) and swollen, thereby the permeate flux increased and dye rejection decreased as shown in Figure 2.6 (Ong et al. 2014).

Zhao et al. (2017) manufactured a positively charged loose NF membrane. Polyethyleneimine (PEI) was reacted with gallic acid and then thermally deposited on the hydrolyzed polyacrylonitrile (PAN) substrate for textile wastewater treatment. They optimized the membrane by varying GA and PEI concentrations and crosslinking temperatures. When the concentration of PEI was increased from 1 wt% to 2 wt%, the membrane skin layer became denser and the permeation flux decreased from 51 L / m² h to 24.5 L / m² h as shown in Figure 2.7. However, the rejection of methyl blue (800 Da) and Congo red (696 Da) did not change significantly despite the change of permeation flux. Therefore, they fixed the PEI concentration at 1 % (Zhao and Wang 2017).

Li et al. (2019) produced a positively charged loose nanofiltration membrane (LNM) by using Tannic acid (TA) and polyethylenimine (PEI) to form crosslinked skin layer onto polyethersulfone ultrafiltration membrane surface with green rapid coating (GRC) process. The membrane was optimized by varying the tannic acid (TA) concentration and the reaction time. When tannic acid concentration was increased from 0.1 to 0.6 g/L, solute permeability increased, meanwhile, the dye rejection stayed stable after TA concentration of 0.2 g/L. Tannic acid led to an improvement of membrane hydrophilicity, resulted in an improvement in solute permeability. By increasing reaction time from 1 min to 30 min, solute permeability was reduced from 73.5 to 28.7 L/m² h bar while dye rejection was increased from 90.1 % to 99.9 % as shown in Figure 2.8 due to formation of a denser layer. 2 g/L PEI, 0.6 g/L TA and 10 min of reaction time were chosen as optimum parameters and resulting membrane was shown to be stable during 10-hour filtration test with 100 ppm Congo Red (99.8 %) and 1000 ppm NaCl (8.4 %) mixture (Li et al. 2019).

2.4.2. Growth of a Layer on a Support

The NF membrane has moved in a different direction with the advances in nanotechnology. Development of nanostructured materials improved hydrophilicity, permeability, selectivity, and mechanical properties of membranes after they are incorporated into membranes.

Zhao et al. (2018) used the chelating tendency of PEI for metal ions which provided in-situ growth of Ni/Co Layered Double Hydroxides (LDH) on commercial PAN UF substrate. They demonstrated that the growth of LDHs on the modified surface significantly increased the permeability without compromising dye rejection. The permeability of the Ni⁺²/Co⁺²/PEI membrane was obtained 14 L/m² h bar that is approximately 3 times higher than the Co⁺²/PEI membrane. This result shows that Co⁺² ion provided more growth for Co/Ni LDHs which created more channels for water and ions permeation. The effect of the metal concentration and growth time of LDH on the rejection performance of the resulting membrane is shown in Figure 2.9. When the Co⁺² concentration was increased from 2 mM/500 mL to 10 mM/500 mL, the permeation flux decreased from 16 L/m² h bar to 10 L/m² h bar while the rejection of methylene blue (319 Da) increased from 53.1 % to 85.3 %. Similarly, when the growth time of LDH was increased from 3 h to 15 h, the permeation flux was reduced from 25.63 L / m² h bar to 9.89 L / m² h bar and the rejection of methylene blue was enhanced by 30 % to 58 %. LDH nanoparticles on the membrane surface were shown to be stable through 30-hour filtration test with 100 ppm Methyl blue (97.9 %) and 1000 ppm NaCl (3 %) mixture. At the same time, a slight reduction in permeate flux was obtained because of the concentration polarization and membrane fouling (Zhao et al. 2018). Yang et al. (2017) developed the metal-organic framework/polymer hybrid membrane. Firstly, polyethylenimine (PEI) molecules and zinc ions were co-assembled on the commercial polyacrylonitrile (PAN) support. By interfacial reaction, zeolitic imidazolate framework-8 particles were in-situ grown in the polyethyleneimine (PEI) layer. They examined the effect of the PEI concentration, reaction time and Zn(NO₃)₂ concentration on the membrane performance. When the interfacial reaction times were elevated from 30 min to 120 min, acid fusion (585 Da) rejection was enhanced from 90.3% to 94.6% while solute permeability was reduced from 60 L / m² h bar to 45.3 L / m² h bar. Increasing zinc nitrate concentration from 0.0 mol/L to 0.1 mol/L resulted in an increase in the acid

fusion rejection from 72.3% to 94.4% and permeability from 12.6 L/ m² h bar to 42.0 L/ m² h bar. This can be attributed to creation of water channels in the presence of ZIF-8 particles (Yang, Wang, and Zhang 2017). The textile wastewater contains a large amount of salt, and the stability of ZIF-8 in the presence of high salt concentration is a main concern (Hermans et al. 2015).

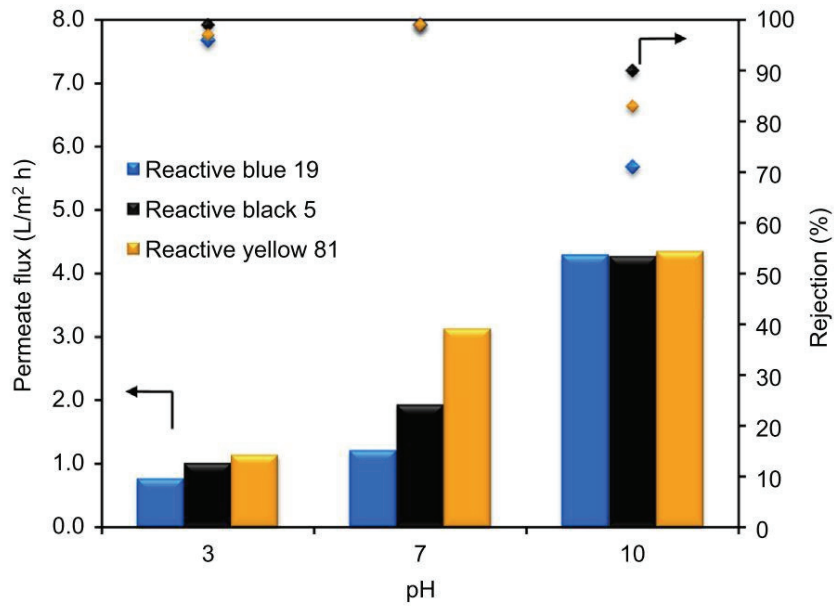


Figure 2.6. Performance of the membrane as a function of pH (100 ppm dye, at 1 bar). (Source: Taken from Ong et al. 2014)

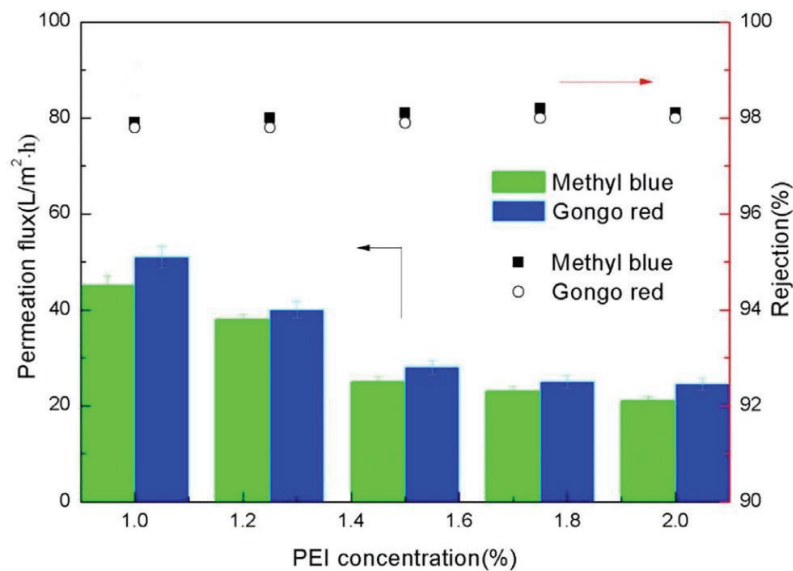


Figure 2.7. The effect of PEI concentrations on the dye rejection and permeation flux of the fabricated membrane (GA concentration: 0.1 wt %, at 2 bar). (Source: Taken from Zhao and Wang 2017)

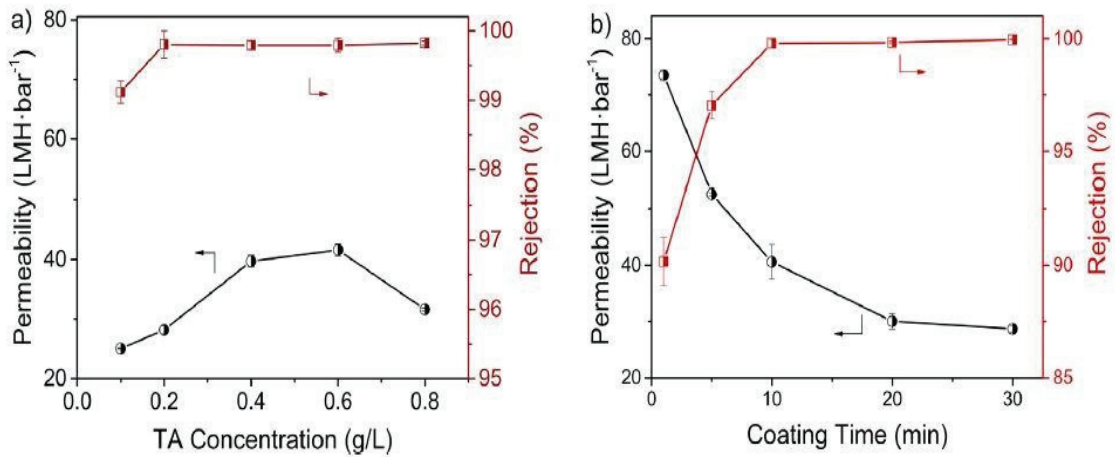


Figure 2.8. Influence of a) Tannic acid concentration and b) coating time on congo red permeability and rejection (Coating conditions: a) 2 g/L PEI and coating time of 10 min; b) 2 g/L PEI and 0.6 g/L TA). (Source: Taken from Li et al. 2019)

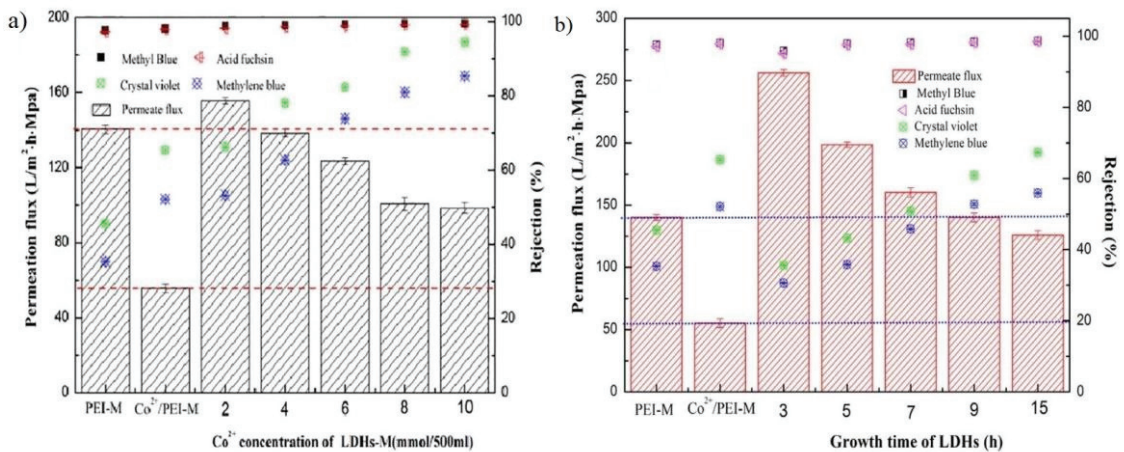


Figure 2.9. The effect of a) the Co²⁺ concentration and b) the growth times of LDHs on membrane performance. (Source: Taken from Zhao et al. 2018)

2.4.3. Surface Modification with Inorganic Compounds

Soyekwo et al. (2017) produced metal-functional nanocomposite NF membrane. Firstly, PEI was crosslinked with glutaraldehyde then grafted on multiwalled carbon nanotubes (MWCNT) interlayer. The resulting membrane was modified by an in-situ surface reaction of Zn(NO₃)₂ with ammonium hydroxide. The effects of reaction time and zinc nitrate concentration on permeability and rejection were investigated. As shown in

Figure 2.10a, a maximum in the permeability and rejection were observed at 50 mM and 100 mM zinc nitrate concentration, respectively. Up to 50 mM, the permeability increased as a result of the increased charge density on the membrane surface, which provided the adsorption of water molecules. Further increase in zinc nitrate concentration decreased the permeability since by the excess $Zn(OH)_2$ blocked the pores.

At low Zn^{2+} concentrations, the formed complex can be stable with excess positive charge that causes more coordination bond between zinc and amine group of the PEI chains. In contrast, at high Zn^{2+} concentrations, the precipitate formed due to the absence of the excess charge group in the environment causes the complex to destabilize, thereby reducing the charge density of the complex. With the elevated reaction time, salt rejection first increased due to attachment of more Zn^{2+} species. On the other hand, at later times, then the PEI chelating agent creates zero-value zinc nanoclusters for the complexation and thus the charge density of the membrane decreased, as a result, salt rejection declined (Soyekwo et al. 2017).

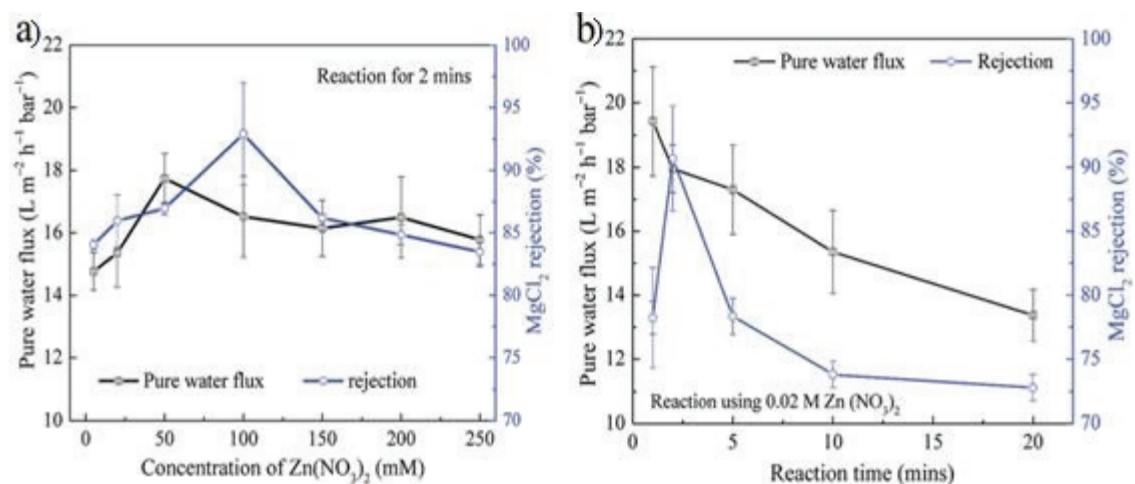


Figure 2.10. The pure water permeability and the salt rejection of the metal-functionalized nanofiltration membrane with different a) $Zn(NO_3)_2$ concentration and b) reaction time. (Source: Taken from Soyekwo et al. 2017)

Figure 2.11 shows the filtration of NaCl and mixture of NaCl and the negatively charged dye (methyl orange) through $Zn(NO_3)_2$ modified membrane. In this case, the rejection of NaCl increases, since the negatively charged dye is adsorbed onto the membrane surface and the membrane pores become smaller, and as a result, the flux drops undesirably. While the rejection of the cationic methylene blue (319 Da) was expected to be higher than anionic dye with the same molecular weight according to the Donnan

exclusion, the flux was reduced due to the high adsorption of the anionic dye (327 Da) on to the membrane surface, and therefore higher rejection was obtained for anionic dye (Soyekwo et al. 2017).

Li et al. (2018) modified the commercial PAN UF substrate in order to produce a positively charged membrane through a coordinated crosslinked layer with the PEI-phosphate -Fe (III) in order. The hydrolyzed PAN substrate was first immersed in PEI then IP6 and finally in FeCl₃ 6H₂O aqueous solution. The membrane was optimized in detail by changing PEI, IP6 and FeCl₃ 6H₂O concentrations. The Fe³⁺ concentration had little influence on the dye rejection as shown in Figure 2.12, on the other hand, IP6 molecules performed a more decisive role throughout the reaction.

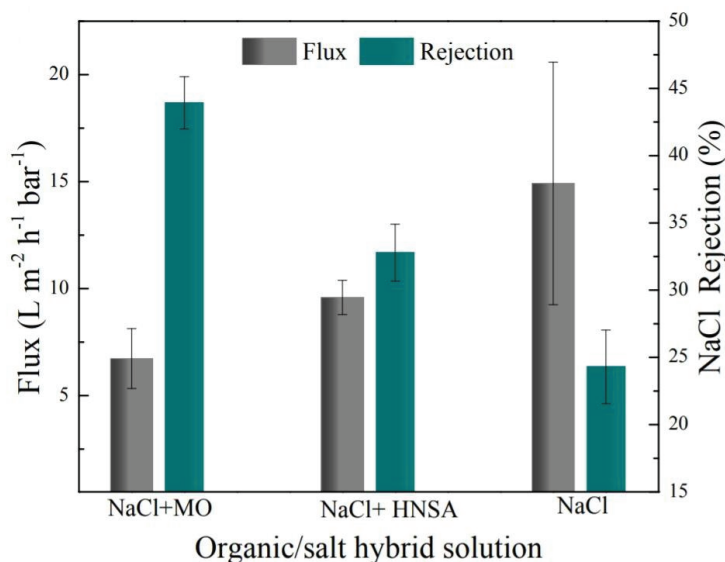


Figure 2.11. The flux and the organic/salt rejection of the metal-functionalized nanofiltration membrane. (Source: Taken from Soyekwo et al. 2017)

After optimization, the long term separation performance of the membrane was evaluated by filtration of model solution that contains Methyl blue (800 Da) and NaCl blend at 2 bar. As shown in Figure 2.13 (a), during the 30 h filtration the rejection of Methyl blue and NaCl was 99.6 % and 8.8 %, respectively. The solute permeation did not change much and it was almost 5 L/ m² h bar. In addition, the actual textile wastewater was filtered through the membrane for 100 hours (Figure 2.13 (b)). The COD removal efficiency of the membrane was about 96 %. However, during the first 10 hours of filtration, the solute permeability dropped dramatically and then remained constant at

about 3 L / m² h bar. They demonstrated that the solute permeation was reduced due to fouling by inorganic salts, dyes, and surfactants in textile wastewater. (Li et al. 2018).

Fan et al. (2015) used the PES substrate to form a stable metal–polyphenol complex on this support. Firstly, the support was soaked into tannic acid (TA) aqueous solution and then immersed into the aqueous solution of FeCl₃ to allow reaction between them. The effect of TA, Fe³⁺ concentration and reaction time on the separation and permeability values of TA-Fe(III)/PES composite NF membranes were investigated. No significant change in pure water flux was observed when the reaction time was increased after the first 1 min as shown in Figure 2.14. This demonstrates that the coating process was completed immediately (Fan et al. (2015)).

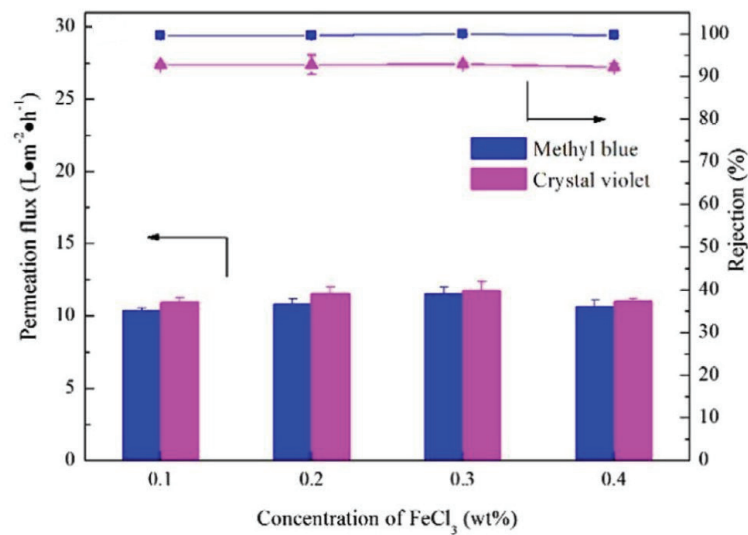


Figure 2.12. The influence of FeCl₃ concentration on the separation performance of the membrane. (Source: Taken from Li et al. 2018)

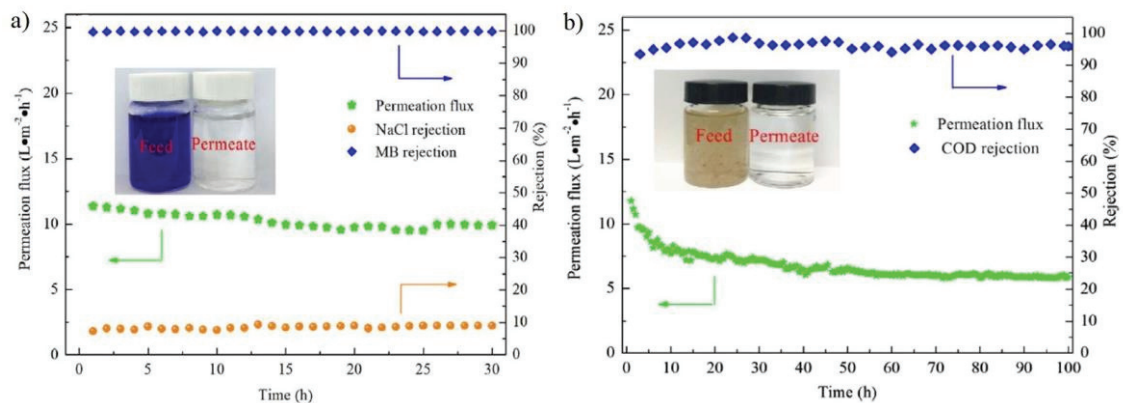


Figure 2.13. Long-term separation performance of the resulting membrane for a) model solution and b) real textile wastewater. (Source: Taken from Li et al. 2018)

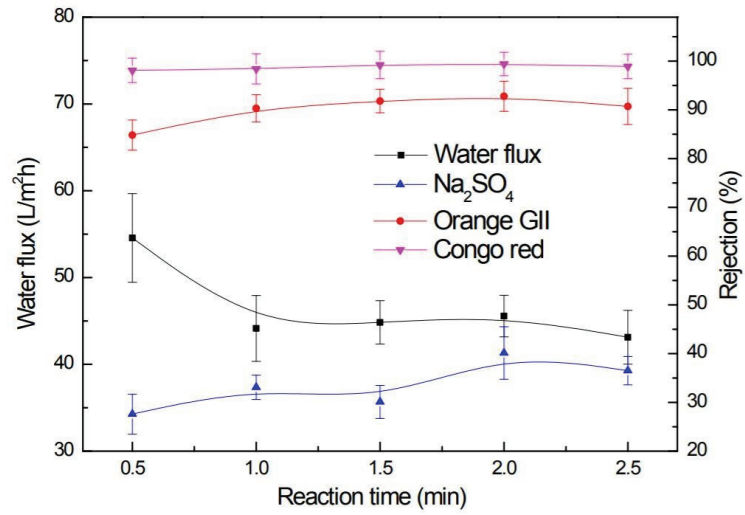


Figure 2.14. The effect of reaction time on dye rejection and pure water flux of the nanofiltration membranes (at 2 bar). (Source: Taken from Fan et al. 2015)

CHAPTER 3

MATERIALS AND METHODS

3.1. Materials

Polyamide-imide (PAI) (Trade name Torlon®, 4000 T-LV) kindly donated by Solvay Advanced Polymers and N-methyl-2-pyrrolidone (NMP, anhydrous, greater than 99.5%) bought from Merck, were used as polymer and solvent during support membrane preparation. Branched polyethyleneimine (PEI) (MW 25 kDa) was purchased from Sigma-Aldrich. Alginic acid sodium salt from brown algae (ALG) (the range of MW of 80-120 kDa), $\text{Zn}(\text{NO}_3)_2 \cdot 6\text{H}_2\text{O}$ and $\text{FeCl}_3 \cdot 6\text{H}_2\text{O}$ were supplied by Sigma Aldrich and Riedel-de Haen, respectively. Sodium chloride (NaCl) was purchased from Sigma-Aldrich. Methylene Blue (319 Da) and Methyl Green (608 Da) were purchased from Sigma Aldrich and Isolab respectively. The real textile wastewater samples were received from 'Ekoten Fabrics' in İzmir, Turkey to test long-term separation performance of the optimized membrane. Figure 3.1 represents the structures of the polymers used in the design of the composite membrane.

3.2. Membrane Preparation

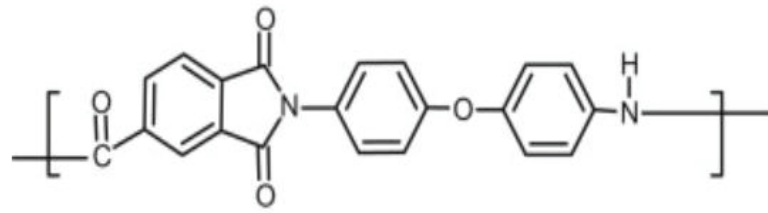
Support membranes were prepared in a single step by phase inversion method, then the resulting membrane was in-situ modified with the alginate and coordinated with the metal ions.

3.2.1. Preparation of Support Membranes by Phase Inversion Method

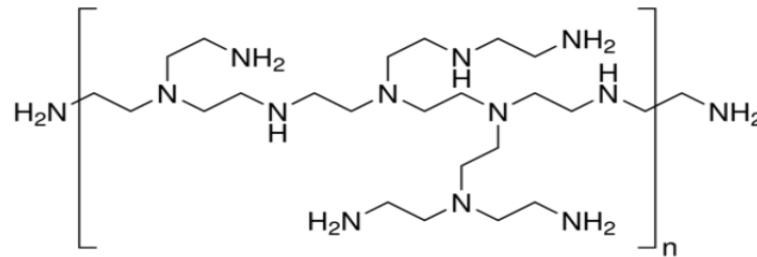
Firstly, polyamide-imide was dried at 177 °C for 3 hours in a vacuum to make sure it was free of moisture. The dried polymer was dissolved in the NMP with stirring at 100 rpm in the Schott bottle. The polymer solution was placed in an oil bath at 70 °C for 18 hours during dissolution process. Then, the polymer solution was left without stirring for 24 hours to remove air bubbles. After degassing, the casting solution was poured onto the glass plate that was coated with nonwoven fabric. The poured solution was cast via an automated film applicator (Sheen Instrument Ltd., model number: 1133N) at room temperature with the help of a knife that has a 200 µm gap size. The casted polymer solution was immersed in a coagulation bath which contains aqueous polyethyleneimine solutions and held in the bath for 18 hours. Afterward, membranes were rinsed thoroughly with deionized water and immersed in deionized water for 24 h to remove loosely bound polyethyleneimine.

3.2.2. Surface Modification of Support Membrane

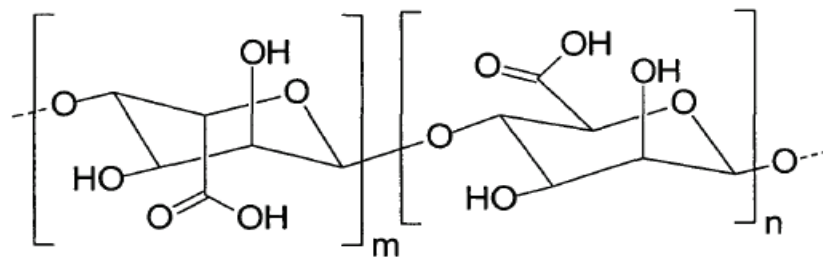
The prepared support membrane was placed between two rubber pieces in order to deposit 1 g/L of alginate solution without further pH adjustment under static conditions, (Figure 3.2). Following alginate-deposition, pure water was filtered through the membrane for about 1 hour at 2 bar. The permeated amount of water was recorded for at least 30 min at 2 bar to calculate pure water permeability of the membrane. Afterward, the metal salt was dissolved in ultrapure water without pH adjustment. The aqueous metal solution was poured into the membrane surface to react with alginate for a certain time. The membranes were then washed thoroughly and water was passed through the membrane about 1 hour at 2 bar. The permeated amount of water was recorded for at least 30 min at 2 bar to calculate pure water permeability of the membrane. The membranes were stored in deionized water at 4 °C until further tests and characterization.



(a)



(b)



(c)

Figure 3.1. Structure of polymers (a) PAI (b) PEI (c) ALG.

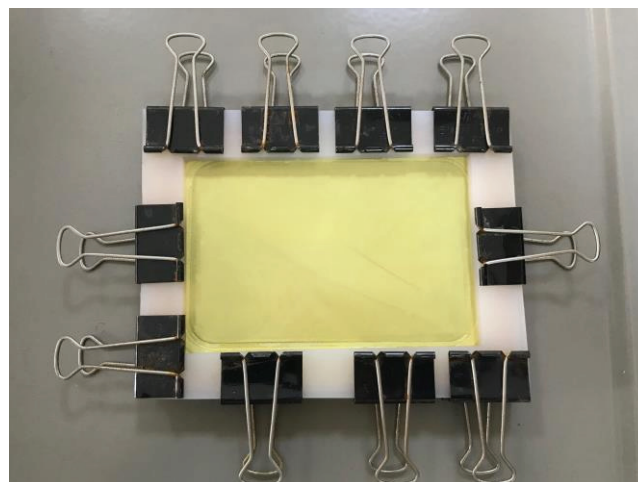


Figure 3.2. Alginate deposition under dynamic condition.

3.3. Filtration Experiment

Filtration experiments consist of pure water flux and rejection measurements are given below.

3.3.1. Water Flux Measurement

Filtration measurements were conducted via using dead-end filtration unit (Sterlitech HP4750 Stirred Cell) which has an effective area of 14.6 cm² and a volume of 300 mL (Figure 3.3). Prior to the actual filtration experiments, each membrane was compacted with distilled water at 3 bar until steady-state conditions were achieved. After compaction, the permeated amount of water was recorded for at least 30 min. at 2 bar in order to calculate flux J_w (L/m² h) and pure water permeability PWP (L/m² h bar) according to the following equations.

$$J_w = \frac{\Delta V}{A \times \Delta t} \quad (3.1)$$

$$PWP = \frac{\Delta V}{A \times \Delta t \times \Delta P} \quad (3.2)$$

Where ΔV (L) is the permeated water volume, A (m²) is the membrane effective area, Δt (h) is the permeation time and ΔP (bar) is the transmembrane pressure difference applied across the membrane. All experiments were performed at room temperature.

3.3.2. Rejection Measurement

During all solute filtration (rejection) experiments, the magnetic stirrer was used to ensure well-mixing and decrease in concentration polarization which may otherwise

take place on the membrane surface. Initial rejection experiments were performed with a single dye solution (methylene blue) of 100 ppm at 300 rpm. Separation experiment was carried out with a mixture that is 100 ppm dye (methylene blue) and 1000 ppm salt (NaCl) (Stirring speed:300 rpm). Dye concentrations were measured via an ultraviolet spectrometer (Perkin Elmer, Lambda 25) and salt concentration was measured by Dionex ICS-5000+ Ion Chromatography (IC). Activated carbon was used to prevent dye contamination of the IC column. All rejection experiments were performed at 2 bar with the same dead-end unit used in filtration experiments.

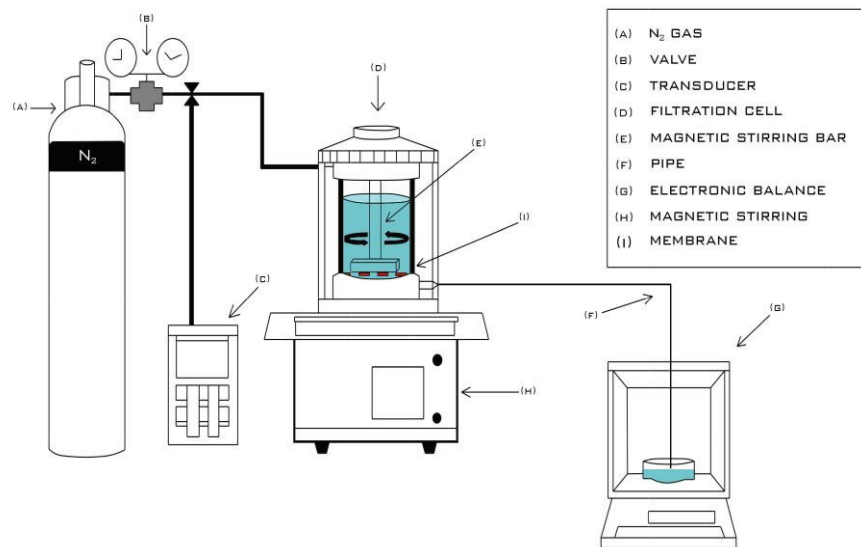


Figure 3.3. Dead-End Unit.

Rejection R (%), selectivity (S_e) and throughput (T) were calculated by using the following equations:

$$R (\%) = \left(1 - \frac{C_p}{C_f} \right) \times 100 \quad (3.3)$$

$$S_e = \frac{100 - R(\%)_{\text{salt}}}{100 - R(\%)_{\text{dye}}} \quad (3.4)$$

Where C_p is the permeate concentration, C_f is the feed concentration,

$R(\%)_{\text{salt}}$ is the salt rejection, and $R(\%)_{\text{dye}}$ is the dye rejection calculated from equation 3.3.

A throughput (T) parameter was calculated from the difference between the S_{salt} and S_{dye} .

$$T = P \times (S_{\text{salt}} - S_{\text{dye}}) \quad (3.5)$$

Where P (L/m² h) is the solute permeability at 1 bar.

$$S_{\text{salt}} = \frac{Cp_{\text{salt}}}{Cf_{\text{salt}}} \quad (3.6)$$

$$S_{\text{dye}} = \frac{Cp_{\text{dye}}}{Cf_{\text{dye}}} \quad (3.7)$$

3.4. Characterization of the Membranes

The modified and unmodified membranes were characterized by Scanning Electron Microscopy (SEM), Energy dispersive X-Ray Analysis (EDX), Zeta Potential, Atomic Force Microscopy and Contact angle measurements.

3.4.1. Atomic Force Microscopy (AFM)

Surface roughness of the membranes was carried out using atomic force microscopy (AFM) (MMSPM Nanoscope 8, Bruker). Scanning was conducted with dried membranes in tapping mode for 10x10 μm² surface using TAP150 model tip.

3.4.2. Scanning Electron Microscopy (SEM)

By using Scanning Electron Microscopy (FEI Quanta 250 FEG), the surface morphology and cross-section image of membranes were obtained. For taking cross-section image, membrane firstly was submerged in liquid nitrogen and then cut with a razor blade. In addition, the elemental composition of the membrane surfaces was determined by Energy Dispersive X-Ray Analysis (EDX) of the same SEM device. All membranes were dried and then coated with gold nanoparticles by Magnetron Sputter Coating Instrument before SEM measurements.

3.4.3. Contact Angle

The membrane hydrophilicity was assessed by using Attension Optical tensiometer. Then membranes were cut in a desirable shape and attached on a glass slide via double-sided tape. Contact angle measurements were taken on the membrane surface at room temperature with 5 μ l volume of the liquid droplet. All membranes were dried to eliminate the humidity in a vacuum oven (Mettler) at 30 °C for 24 h prior to analysis.

3.4.4. Zeta Potential

The surface charge of membranes was analyzed in the existence of a 10 mM NaCl solution by a NanoPlus Micromeritics Instrument. The electrolyte solution was arranged by using HCl and NaOH for acidic and basic pH, respectively. The streaming potential measurements were performed 3 times at 4 different pH which is 3.0, 5.0, 7.0, 9.0 and 11.0.

3.4.5. Stability Test

The stability of the optimized membrane was analyzed by storing in 1 M NaCl solution under static conditions. After 12 days, the sample was taken from the NaCl solution where the membrane was stored to determine the amount of metal release from the membrane surface. Inductively Coupled Plasma Mass Spectrometer (Agilent 7500ce Octopole) was used to determine the iron amount in the aqueous sample.

3.4.6. Long Term Separation Performance

All long-term experiments were conducted using a cross-flow filtration unit shown in Figure 3.4. Cross-flow filtration unit has an effective area of 150 cm² and a volume of 3 L. Prior to the actual filtration experiments, each membrane was compacted with distilled water at 3 bar until steady-state conditions were achieved. After compaction, the permeated amount of water was recorded for at least 30 minutes at 2 bar.

The long-term separation performance was carried out with real textile wastewater or a model mixture that contains 100 ppm dye (methyl green) and 1000 ppm salt (NaCl) for 72 h at 2 bar. For the model solution, samples were collected at regular intervals during the filtration. From the collected samples, dye and salt concentrations were measured via an ultraviolet spectrometer (Perkin Elmer, Lambda 25) and Dionex ICS-5000 ion chromatography (IC), respectively. Activated carbon was used to prevent dye contamination of the IC column. For real textile wastewater treatment, membrane performance was characterized by measuring the TOC, TSS, TDS, COD, color, pH and conductivity parameters before and after treatment using devices listed in Table 2.1.

Table 3.1. Devices for measurement of real textile wastewater parameters.

Parameters	Devices
TOC	Shimadzu TOC-VCPH
TSS	SM 2540 D
TDS	OAKTON Waterproof TDS Testr11
COD	HACH LANGE LT 200
Color	HACH DR 600
Conductivity	Oakton Waterproof ECTestr 11+
pH	HANNA HI198127



Figure 3.4. Crossflow filtration unit.

CHAPTER 4

RESULTS AND DISCUSSION

4.1. Preparation of Support Membranes by Phase Inversion Method

Membranes can be transformed from a highly porous to a very dense non-porous structure by altering important factors affecting phase inversion membrane formation, such as the choice of solvent non-solvent system, the composition of the casting solution and, the composition of the coagulation bath (Mulder 1997).

Selectivity and pure water permeability are the main characteristics that determine the performance of a membrane. Although high flux membranes are often accompanied by low selectivity and vice versa, it has always been intended to achieve both high permeability (flux) and high selectivity (retention).

The main objective of this thesis is to develop positively charged nanofiltration membrane that has high permeability and selectivity (throughput) for the separation of dyes and salts in textile wastewater treatment.

4.1.1. Effect of Coagulation Bath Composition

The composition of coagulation bath has a significant influence on the final membrane morphology through controlling the precipitation rate. The sponge-like and finger-like structure can be produced with a slow and fast precipitation rate, respectively. Unlike the finger-like membrane structure, the sponge-like membrane has low water fluxes with high rejection (Guillen et al. 2011). The goal is to optimize this inverse relationship between flux and rejection by altering the coagulation bath composition.

The support membrane used in this study was developed by adding polyethylenimine (PEI) in the coagulation bath. The amine groups of PEI form a chemical

crosslink with imide groups of Polyamideimide (PAI) as shown in Figure 4.1. When the PEI concentration in the coagulation bath was increased from 0.25 (wt %) to 0.75 (wt %), pure water permeability decreased from 11.21 L/ m² h bar to 6.76 L/ m² h bar as shown in Figure 4.2. The selectivity performances of the membranes prepared at the lowest and highest PEI concentration, denoted as membranes A and C, were evaluated by filtration of methylene blue (100 ppm) and NaCl (1000 ppm) mixture at pH 3. The membrane surface becomes more protonated at lower pH, therefore, the filtration was carried out at pH 3 in order to get more benefit from the Donnan exclusion mechanism of the membrane. Increasing the PEI content from 0.25% to 0.75 % resulted in an increase in dye rejection from 74.94 % to 82.16 % and salt rejection from 30.93 % to 48.21 %. The results indicated that the dye rejection should be enhanced while the salt rejection should be decreased to achieve better separation of the dye and salt in water.

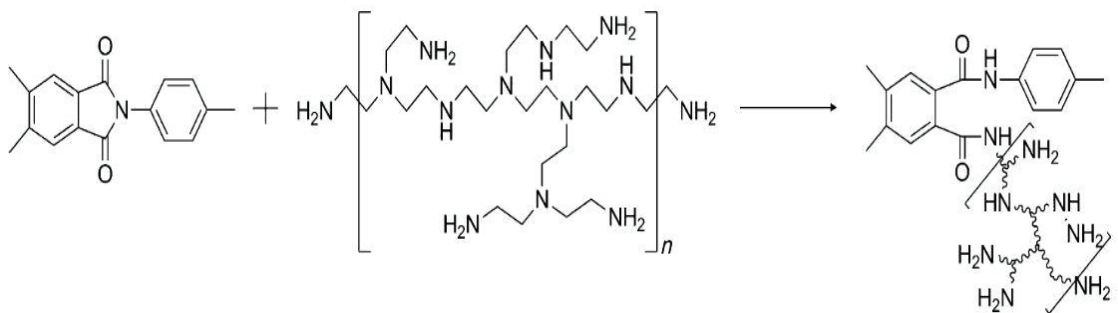
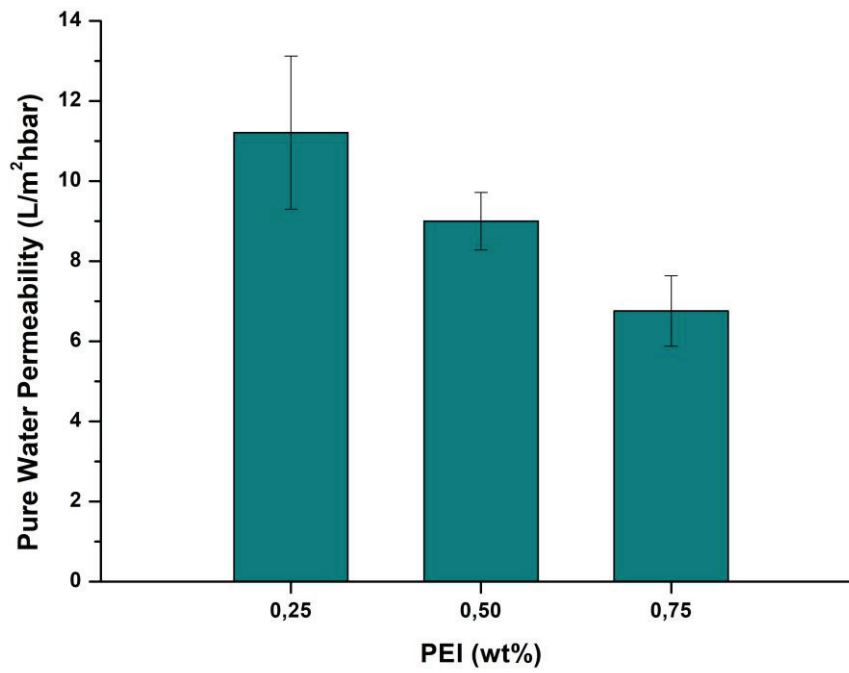


Figure 4.1. The crosslinking reaction between PAI and PEI.
(Source: Taken from Li et al. 2013)

Table 4.1. Casting conditions for the support membranes.

Membrane	Polymer		Membrane Thickness (μm)	Coagulation Bath Composition (wt %)
	Concentration (wt %)	Solvent		
A	20	NMP	200	0.25
B	20	NMP	200	0.5
C	20	NMP	200	0.75

a)



b)

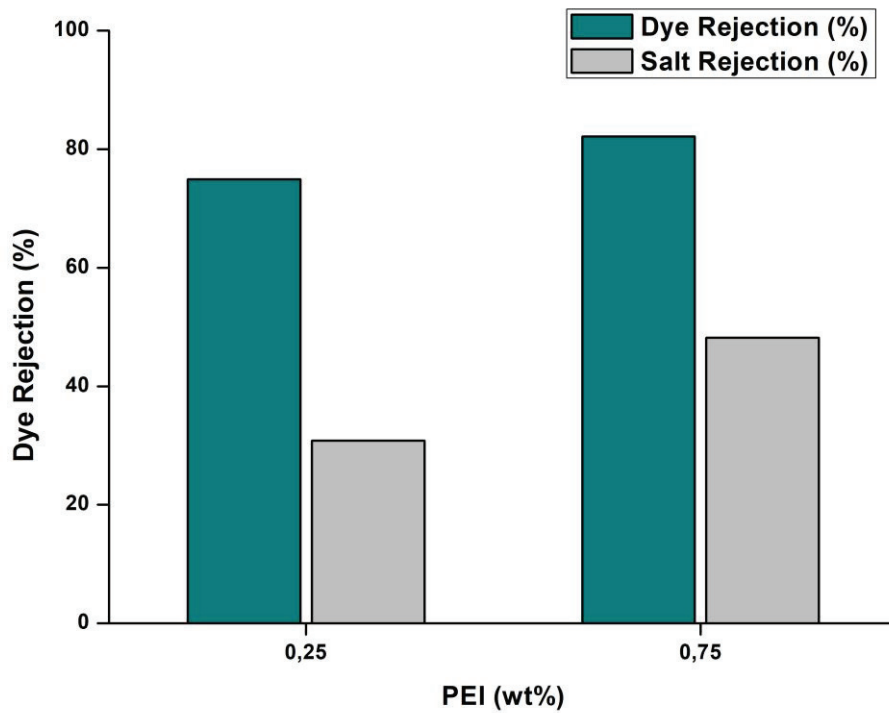


Figure 4.2. The effect of PEI concentration on a) the pure water permeability (PWP) and b) dye and salt rejection (pH3).

4.1.2. Effect of Polymer Concentration

Polymer concentration is another significant parameter that affects the membrane morphology. The increased polymer concentration in the casting solution results in a more dense structure on the surface with a lower overall porosity (Guillen et al. 2011).

The polymer concentration in the casting solution was changed from 15 % to 20 %. Below 15 %, it was not possible to obtain a continuous layer on the nonwoven. The results have shown that upon increasing the polymer concentration from 15 % to 20 %, the pure water permeability (PWP) decreased from 15.9 L/ m² h bar to 11.2 L/ m² h bar without significant improvement in dye rejection.

Table 4.2. Casting conditions for the support membranes.

Membrane	Coagulation Bath		Membrane Thickness (μm)	Polymer Concentration (wt %)
	Composition (wt %)	Solvent		
A	0.25	NMP	200	20
D	0.25	NMP	200	18
E	0.25	NMP	200	15

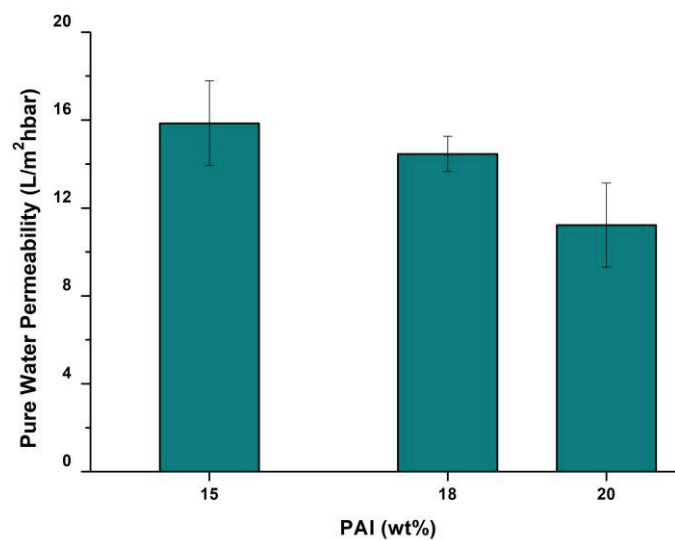


Figure 4.3. The effect of PAI concentration on the pure water permeability.

4.2. Surface Modification of Prepared Membranes with Zinc Nitrate

Changing the coagulation bath and casting solution composition did not produce improved separation performance, therefore, it was decided to modify the membrane surface using inorganic compounds.

PEI has an unshared pair of electrons on the nitrogen atom which has a strong affinity to form donor bonds by coordination of metal ions (Ruey-Shin and Ming-Nan 1996). Zn^{2+} is one of the metal ions that can form a complex with PEI (Saburo, Shoji, and Yukio 1957). In view of this information, the bare membrane surface was decided to be functionalized by in-situ surface reaction of Zn^{2+} ion to form a complex with amine groups in PEI as illustrated in Figure 4.4. $Zn(NO_3)_2 \cdot 6H_2O$ was dissolved in ultra-pure water. Then this metal solution was poured onto the support membrane surface. The membrane prepared with 20 % PAI in the casting solution and 0.25 % PEI in the coagulation bath (Membrane A) was chosen as the support membrane. Literature studies have shown that the metal concentration and reaction time are very effective parameters to control the pore size on the surface (Zhao et al. 2018). The concentration of zinc nitrate and reaction time were optimized according to the methylene blue (MB, MW: 319 Da) rejection performance of the resulting membrane. When the reaction time was increased from 3 min to 10 min, more Zn^{2+} ions attached to the amine groups to form a complex on the membrane surface which resulted in an increase in dye rejection from 93.3 % to 97.3 % and the solute permeability from 6.8 L/m² h bar to 7.9 L/m² h bar respectively, as shown in Figure 4.5.

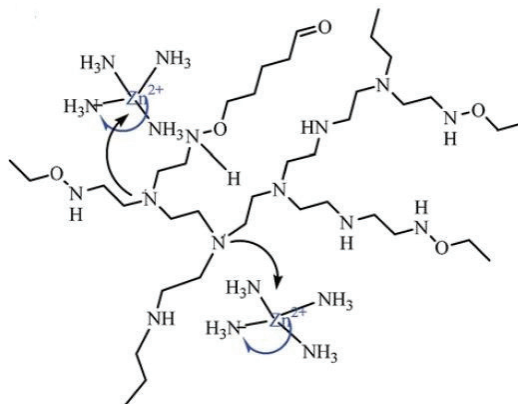


Figure 4.4. The illustration of the coordination mechanism between PEI and Zn^{2+} .
(Source: Taken from Soyekwo et al. 2017)

Table 4.3. Surface modification conditions with Zn(NO₃)₂.

Membrane	Polymer Concentration (wt %)	Coagulation Bath Composition (wt %)	Zn(NO ₃) ₂ Concentration (mM)	Reaction Time (min)
A	20	0.25	2	3
A	20	0.25	2	10

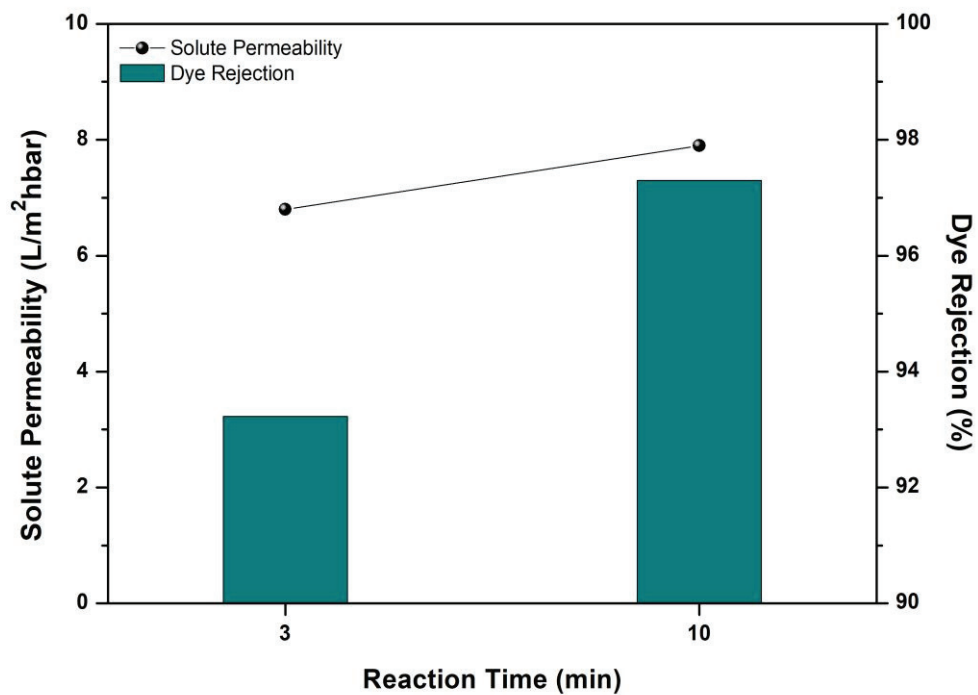


Figure 4.5. Effect of reaction time on dye rejection and permeability performances of membrane A.

When the metal concentration was increased from 2 mM to 10 mM, more Zn²⁺ bounded to amine groups on the surface and consequently the methylene blue rejection increased due to enhanced Donnan exclusion effect as shown in Figure 4.6.

Table 4.4. Surface modification conditions with Zn(NO₃)₂.

Membrane	Polymer Concentration (wt %)	Coagulation Bath Composition (wt %)	Reaction Time (min)	Zn(NO ₃) ₂ Concentration (mM)
A	20	0.25	10	2
A	20	0.25	10	10

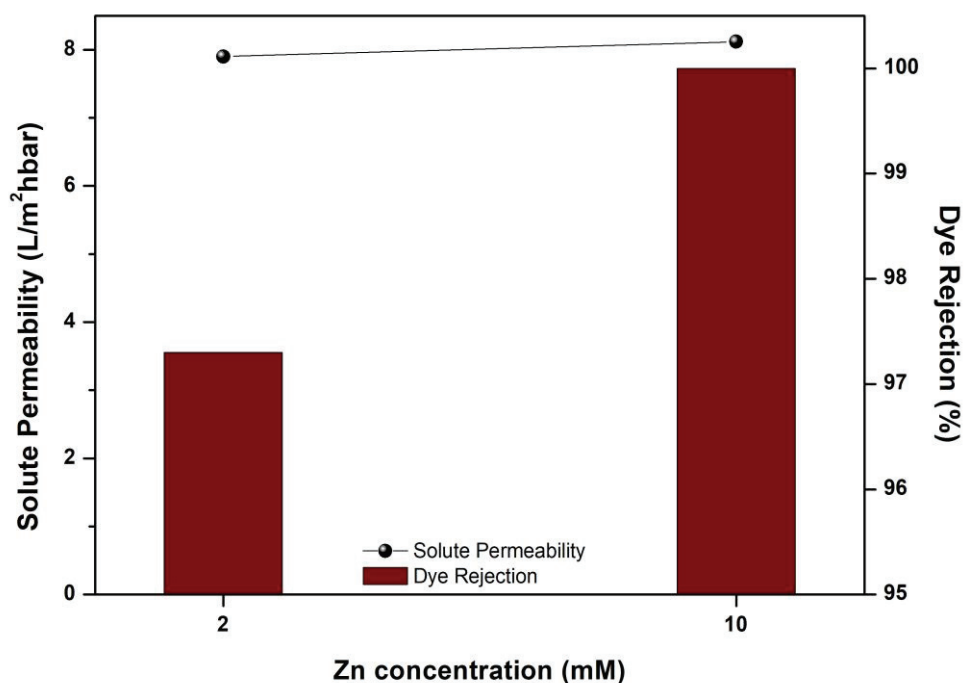


Figure 4.6. Effect of Zn²⁺ concentration on dye rejection and permeability performances of membrane A.

To increase the permeability of the modified membrane, the support membrane prepared with 18 % PAI was exposed to 10 mM zinc nitrate solution for 10 and 20 minutes. Although 100 % of dye rejection was observed by increasing the reaction time from 10 to 20 minutes, a slight decrease in the permeability was observed, in addition, the permeability value less than 10 L/m² h bar was found not satisfactory (Figure 4.7).

Table 4.5. Surface modification conditions with Zn(NO₃)₂.

Membrane	Polymer Concentration (wt %)	Coagulation Bath Composition (wt %)	Zn(NO ₃) ₂ Concentration (mM)	Reaction Time (min)
D	18	0.25	10	10
D	18	0.25	10	20

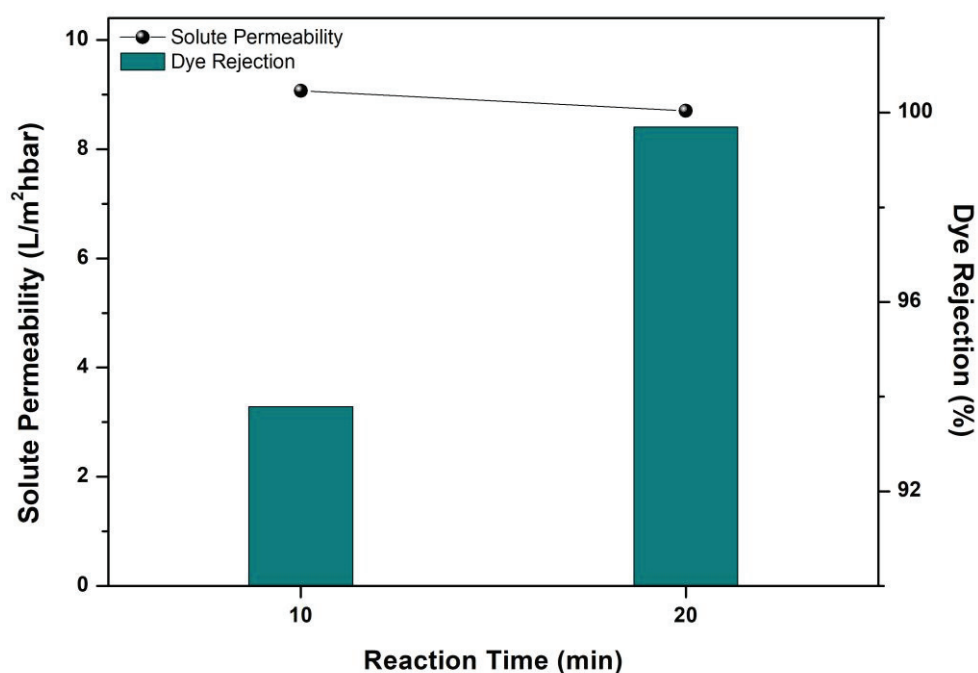


Figure 4.7. Effect of reaction time on dye rejection and permeability performances of membrane D.

In order to increase the PWP, the support membrane prepared with 15 % PAI was modified (Table 4.6) When the reaction time was increased from 20 min to 960 min, the dye rejection did not change significantly as shown in Figure 4.8, therefore, the optimum time for the 10 mM zinc nitrate concentration was determined as 20 minutes. Figure 4.9 illustrates that the methylene blue rejection (94.8 %) did not change when the zinc nitrate concentration was increased from 10 mM to 50 mM. This simply indicated that all the amine groups are saturated at the zinc nitrate concentration of 10 mM, therefore, this concentration was chosen as optimum value.

Table 4.6. Surface modification conditions with Zn(NO₃)₂.

Membrane	Polymer Concentration (wt %)	Coagulation Bath Composition (wt %)	Zn(NO ₃) ₂ Concentration (mM)	Reaction Time (min)
E	15	0.25	10	20
E	15	0.25	10	60
E	15	0.25	10	960

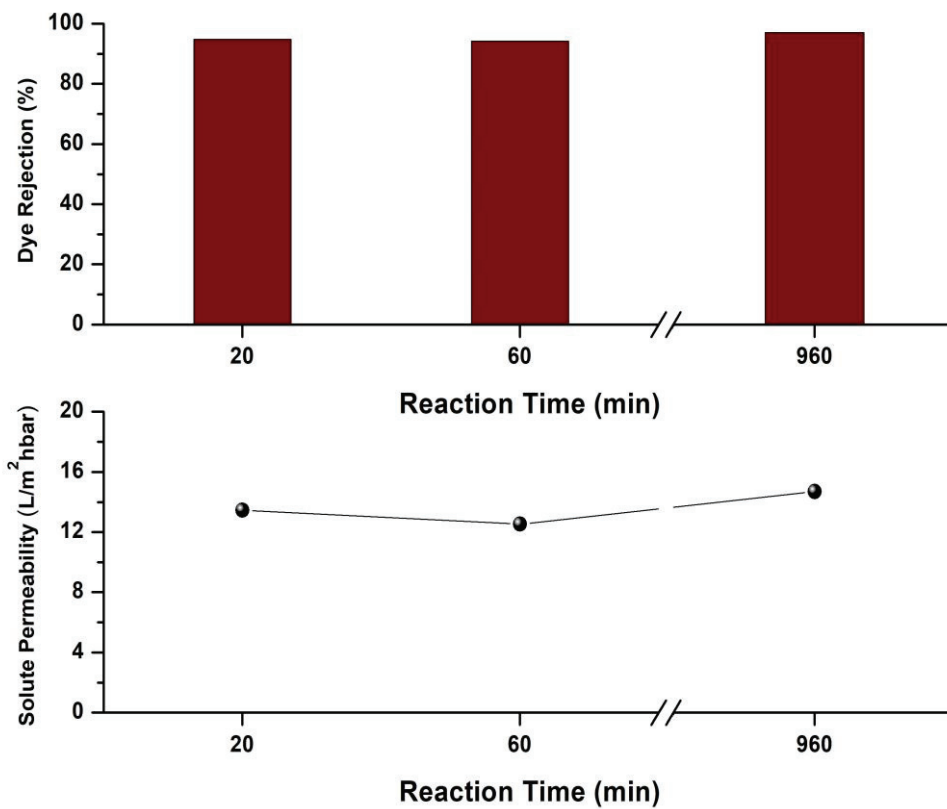


Figure 4.8. Effect of reaction time on permeability and dye rejection performances of membrane E.

Table 4.7. Surface modification conditions with Zn(NO₃)₂.

Membrane	Polymer Concentration (wt %)	Coagulation Bath Composition (wt %)	Reaction Time (min)	Zn(NO ₃) ₂ Concentration (mM)
E	15	0.25	20	10
E	15	0.25	20	50

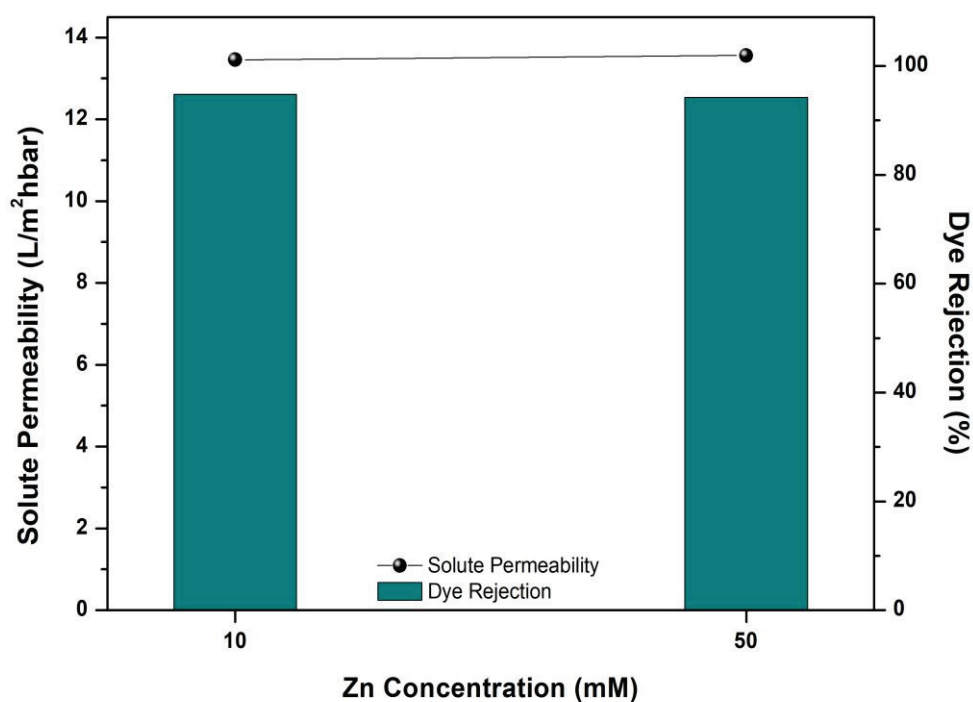


Figure 4. 9. Effect of Zn²⁺ concentration on dye rejection and permeability performances of membrane E.

Figure 4.10 shows that the modification of the support membrane, PAI/PEI (membrane E), by exposing to 10 mM zinc nitrate solution for 20 minutes increased the

methylene blue rejection from 59% to 94% without significantly changing the permeability. In order to check the stability of the zinc nitrate on the surface, the methylene blue/NaCl mixture was filtered through the modified membrane. The dye rejection decreased to approximately 59% while the salt rejection was determined as 11.6%. The results have shown that in the presence of salt all the zinc on the surface released in the form of $ZnCl_2$ since the dye rejection value returned to the value reported for the bare support membrane.

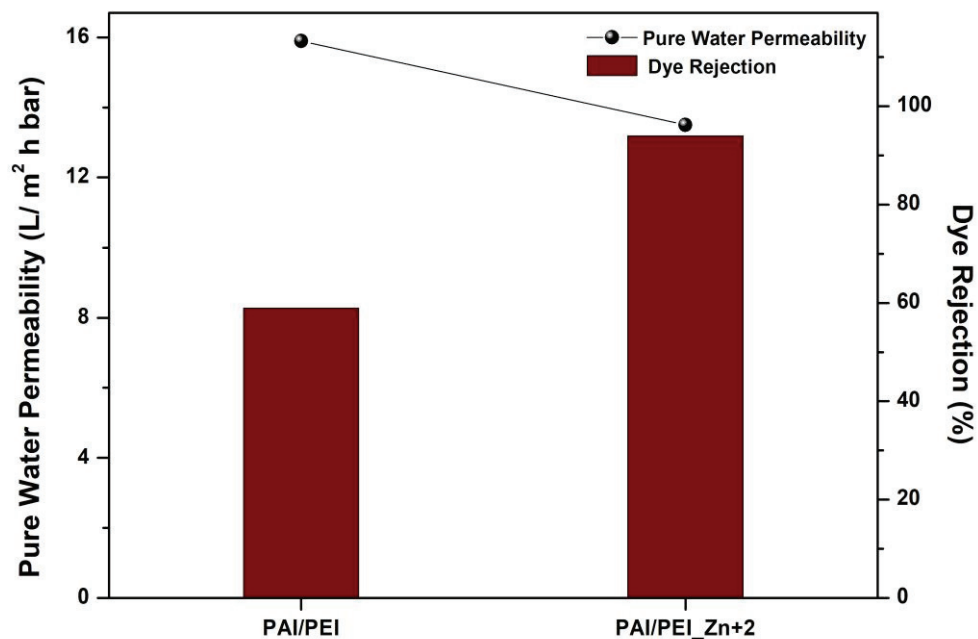


Figure 4.10. Methylene Blue rejection performance of PAI/PEI membrane (bare) and PAI/PEI- Zn^{+2} (modified) membrane.

4.3. Surface Modification of Prepared Membranes with Alginate

As a second strategy for surface modification, the support membrane was first coated with alginate that contains carboxyl groups which can form strong ionic crosslink

with the amine groups in PEI on the support membrane surface as shown in Figure 4.11 (Li, Si, et al. 2018)

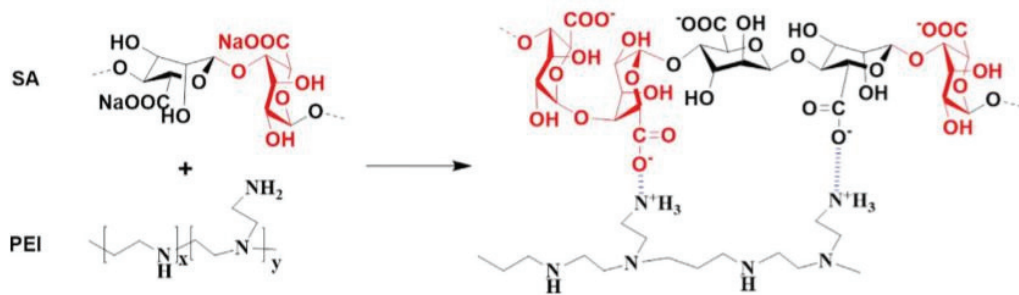


Figure 4.11. Reaction mechanism between PEI and Alginate.
(Source: Taken from Li et al. 2018)

Following alginate deposition, the surface was further modified with a divalent and trivalent cations under static conditions. Alginate is expected to bind to the divalent cations in a planar two-dimensional manner, while the trivalent cation is expected to form a three-dimensional valent bonding structure with the alginate as shown in Figure 4.12 (Al-Musa, Fara D., and Badwan 1999).

The alginate coated membrane was first modified according to the previously optimized conditions for Zn attachment (concentration: 10 mM and reaction time: 20 min). To prove whether there is metal release or not after alginate deposition, the methylene blue was filtered through the membrane (PAI/PEI/Alginate/Zn⁺²) for 1 hour and the dye rejection was determined as 97 %. Next, 1000 ppm NaCl solution was filtered through the dye-filtered membrane, and finally, the dye was re-filtered and the rejection was found to be the same. The result simply indicated that there was no metal release from the membrane.

As a divalent and trivalent cations, Zn⁺² and Fe⁺³ were selected. First of all, 10 mM Zn⁺² and Fe⁺³ aqueous solutions were poured onto the alginate-deposited membrane and kept there for 20 min. To evaluate the performance, 100 ppm methylene blue and 1000 ppm NaCl mixture was filtered through these membranes at 2 bar. The dye rejections of 67 % and 77 % and the salt rejections of 27 % and 30.6 % were obtained for the Zn-modified and Fe-modified membranes, respectively as shown in Figure 4.13. The dye and salt rejection performance of the Zn and Fe-modified membranes are different due to the charge density of the metal ions (Geoff Rayner-Canham 2014). When the

reaction time and metal ion concentration were increased from 20 minutes to 120 minutes and from 10 mM to 50 mM, respectively, the dye rejection values increased from 67% to 81.50% for the Zn-modified membrane and, from 77% to 91% for the Fe-modified membrane. The salt rejection values also increased to 37% and 39% for the Zn-modified and the Fe-modified membranes, respectively, as shown in Figure 4.14. Based on these data, the optimum reaction conditions were determined as 120 minutes and a Fe^{3+} concentration of 50 mM.

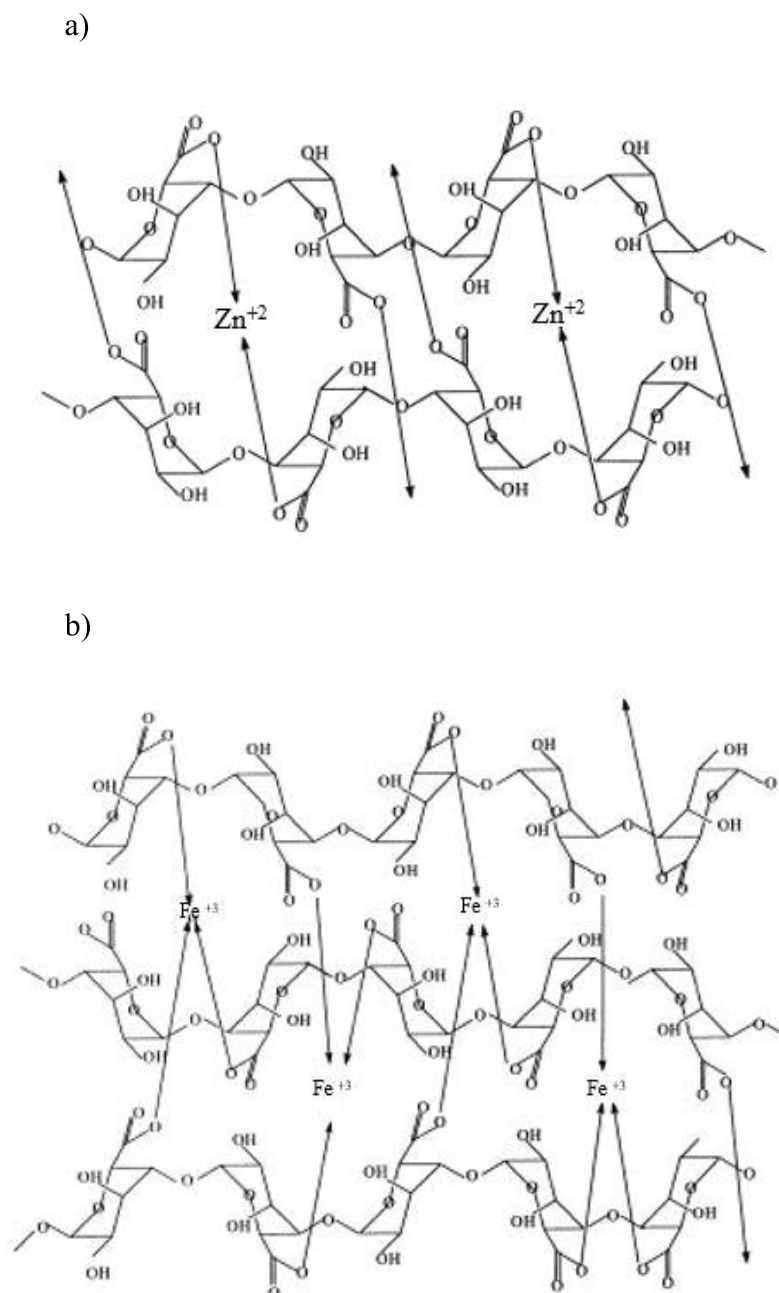


Figure 4.12. Reaction mechanism between a) zinc or b) iron cations with alginate.

Table 4.8. Reaction Condition of Membrane E

Membrane	Polymer Concentration (wt %)	Coagulation Bath Composition (wt %)	Alginate Concentration (g/L)	Reaction Time (min)	Zinc Nitrate Concentration (mM)	Metal Type
E	15	0.25	1	20	10	Zn ²⁺
E	15	0.25	1	20	10	Fe ³⁺

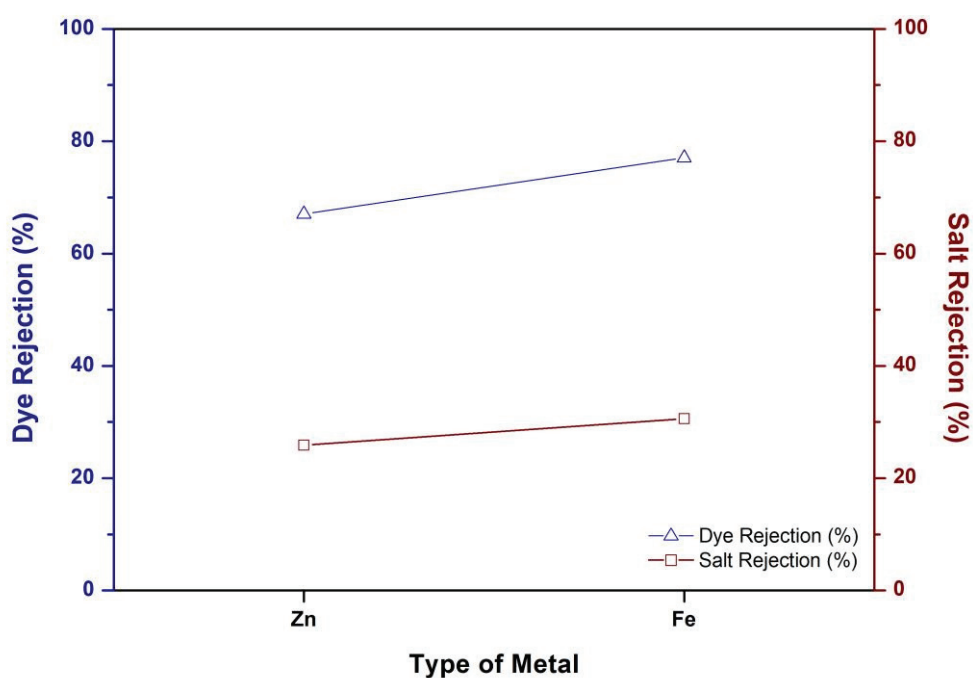


Figure 4.13. Effect of different metal ions on dye rejection and salt rejection performance (reaction time: 20 min, metal concentration: 10 mM).

Table 4.9. Reaction Condition of Membrane E

Membrane	Polymer Concentration (wt %)	Coagulation Bath Composition (wt %)	Alginate Concentration (g/L)	Reaction Time (min)	Zinc Nitrate Concentration (mM)	Metal Type
E	15	0.25	1	120	50	Zn ²⁺
E	15	0.25	1	120	50	Fe ³⁺

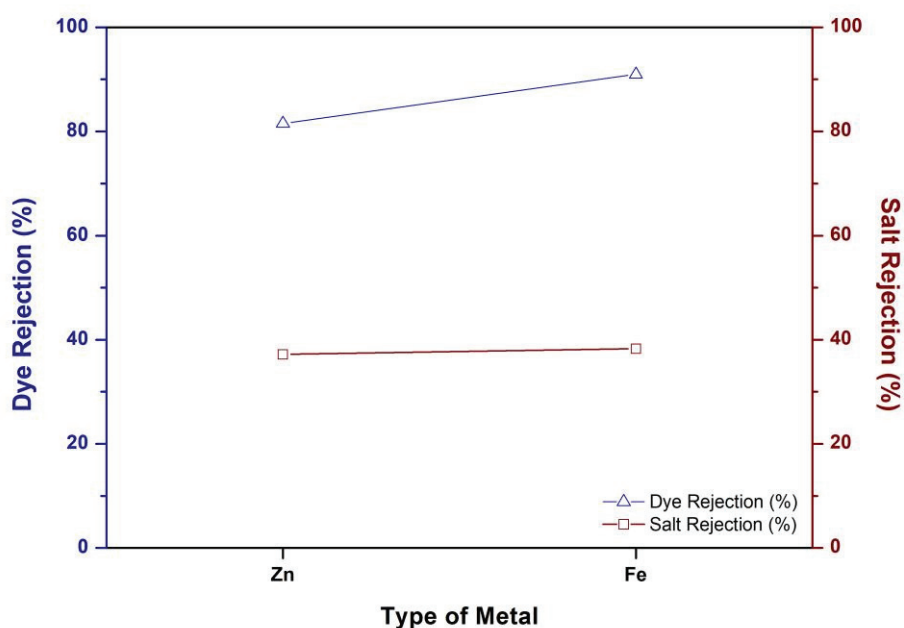


Figure 4.14. Effect of different metal ions on dye rejection and salt rejection performance (reaction time: 120 min-metal ion concentration: 50mM).

The surface charges of bare (PAI/PEI) and modified (PAI/PEI/Alginate/Fe³⁺) membranes were determined by zeta potential measurement. Figure 4.15 shows that the isoelectric point of the bare membrane shifted from pH 6 to pH 10.3. This shift is greatly in favor of the use of Donnan exclusion in the removal of cationic dye from the textile wastewater that exhibit a wide pH range.

EDX analysis results in Table 4.10 demonstrated that after modification of bare membrane, the content of oxygen increased from 17.85% to 20.75% due to alginate deposition. The iron content of 9.53 % confirmed that Fe³⁺ is coordinated onto the surface. Furthermore, the SEM images given in Figure 4.17 prove that the bare membrane surface has been modified.

Table 4.10. EDX analysis of the bare (PAI/PEI) and modified (PAI/PEI/Alginate/Fe³⁺) membranes.

Membranes	C (wt %)	N (wt %)	O (wt %)	Fe (wt %)
Bare membrane (PAI/PEI)	66.32	15.83	17.85	-
Modified membrane (PAI/PEI_Alg_Fe ³⁺)	52.64	13.16	24.67	9.53

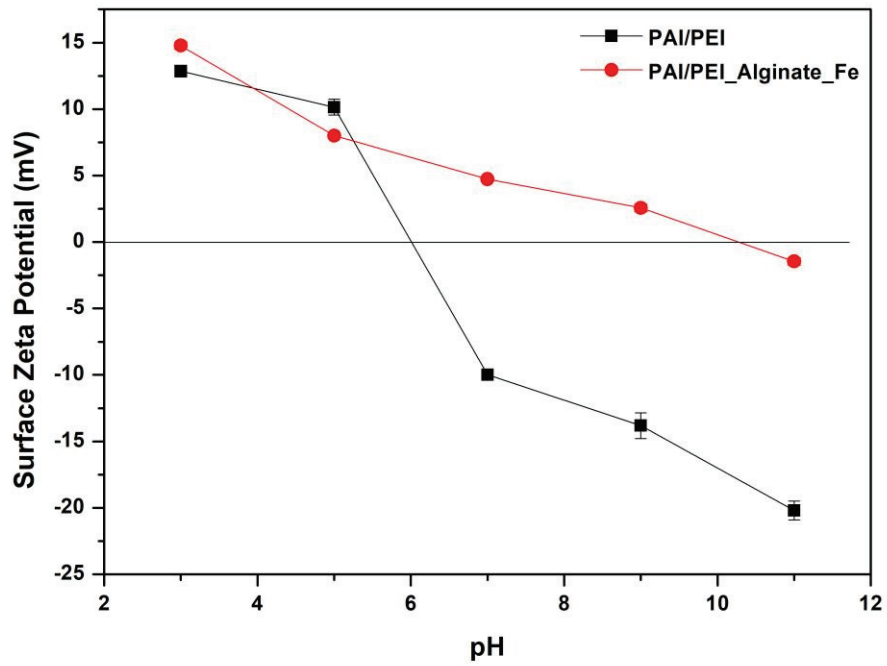


Figure 4.15. Zeta potential as a function of pH for bare membrane (PAI/PEI), modified membrane (PAI/PEI/Alginate/Fe³⁺).

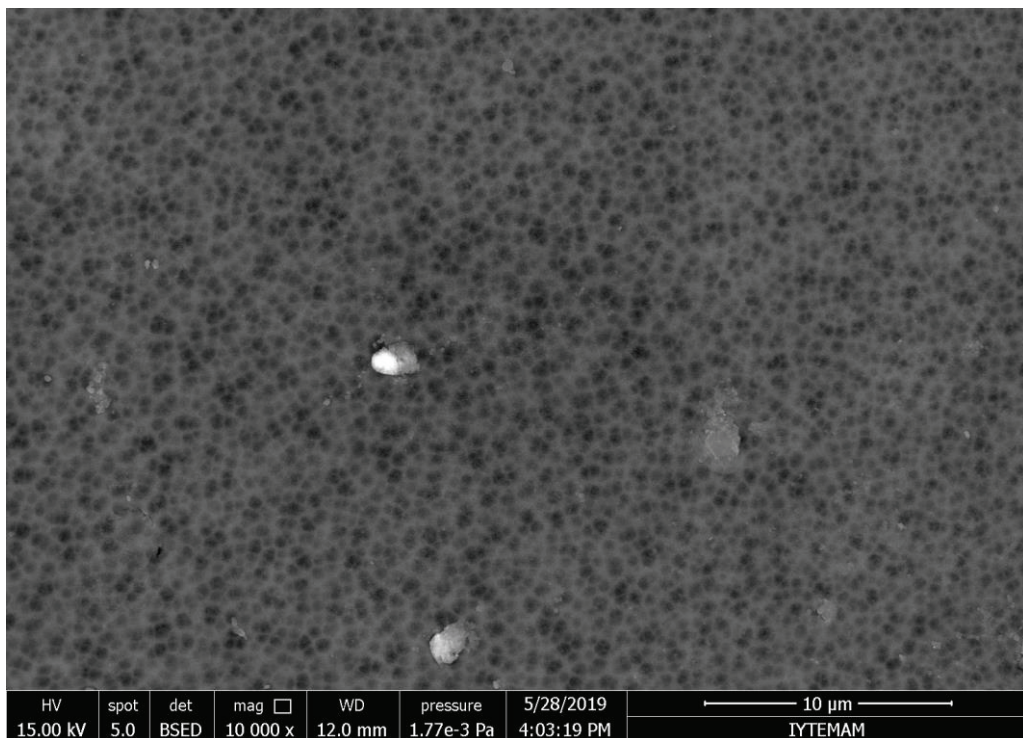


Figure 4.16. Surface SEM images of the bare membrane (PAI/PEI) with magnification 10000x.

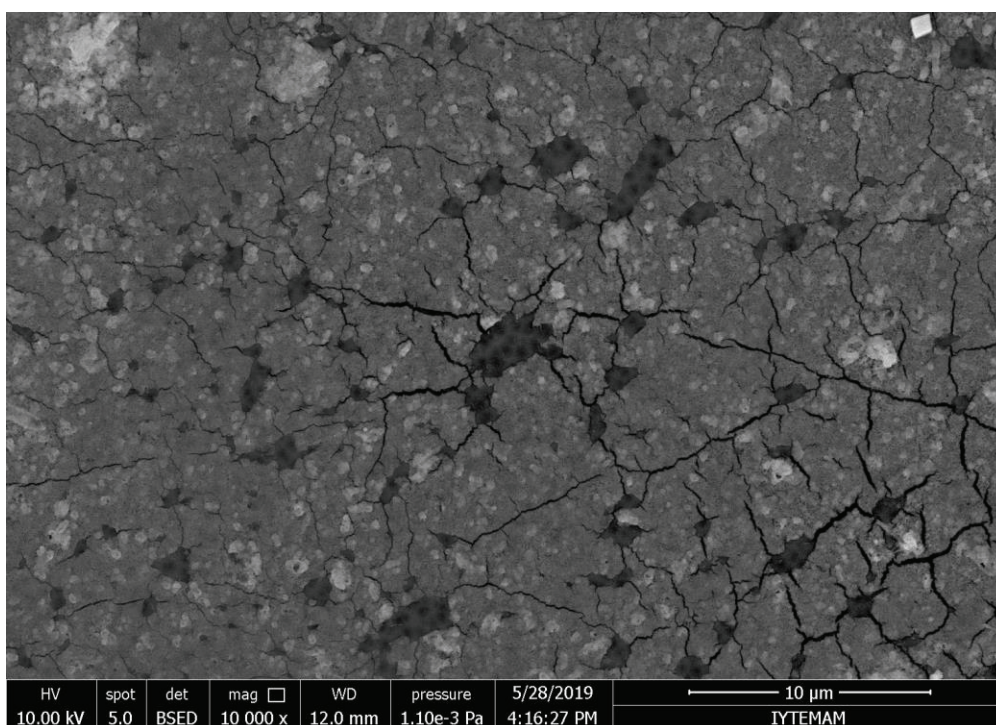


Figure 4.17. Surface SEM images of the modified membrane (PAI/PEI/Alginate/Fe³⁺) with magnification 10000x.

The stability of the optimized membrane was evaluated by storing in 1 M NaCl solution under static conditions. After 12 days of storage, the sample was taken from the NaCl solution and the amount of iron released from the membrane was determined as 16 ppb/cm². This very low value demonstrated that the amount of iron released from the membrane was negligible.

4.4. Long-Term Stability Performance

Figure 4.19 shows the contact angles of the bare and modified membranes. The hydroxyl groups in alginate reduced the contact angle, hence, enhanced the surface hydrophilicity. On the other hand, the hydrophilicity of the PAI/PEI/Alginate/Fe³⁺ membrane was found lower than that of the PAI/PEI/Alginate membrane since the coordination of Fe³⁺ covered some of the hydroxyl groups in alginate as shown in Figure 4.12b. Although the surface became more hydrophilic after alginate deposition, the PWP

of the support membrane decreased from 20.5 L/m² h bar to 16.8 L/m² h bar (Figure 4.18) which can be attributed to the narrowing of the pores. In contrast, the PWP increased to 26.3 L/m² h bar after being coordinated with Fe³⁺ ions and the contact angle measurement did not support this result. This increase in the PWP was correlated with the increase in surface roughness compared to the bare and alginate deposited membranes as given in Figure 4.20-4.22.

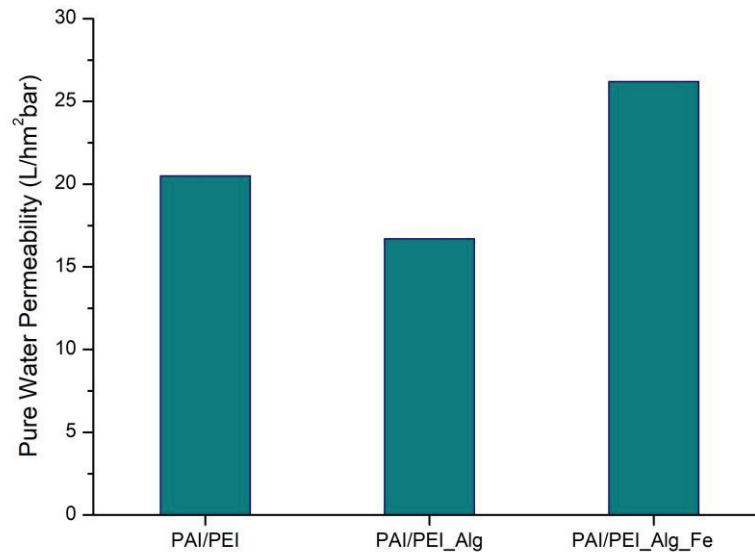


Figure 4.18. Permeability of the bare membrane (PAI/PEI), alginate deposited membrane (PAI/PEI/Alginate) and, resulted membrane (PAI/PEI/Alginate/ Fe³⁺).

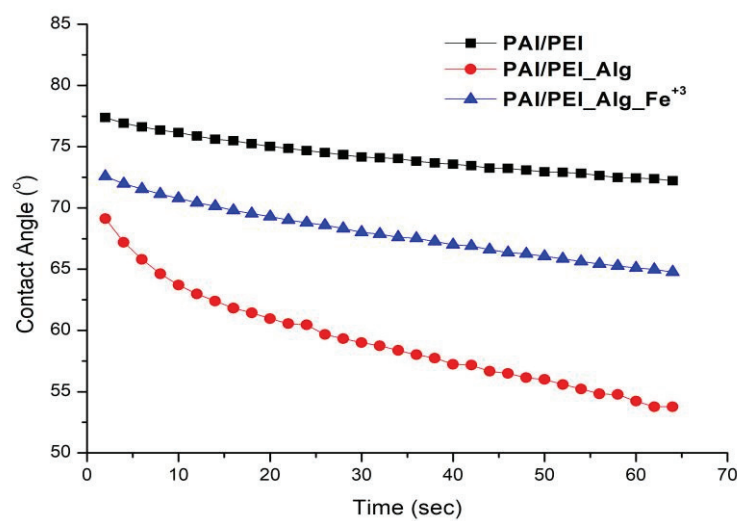


Figure 4.19. Water contact angle of bare membrane (PAI/PEI), alginate deposited membrane (PAI/PEI/Alginate) and, resulted membrane (PAI/PEI/Alginate/ Fe³⁺).

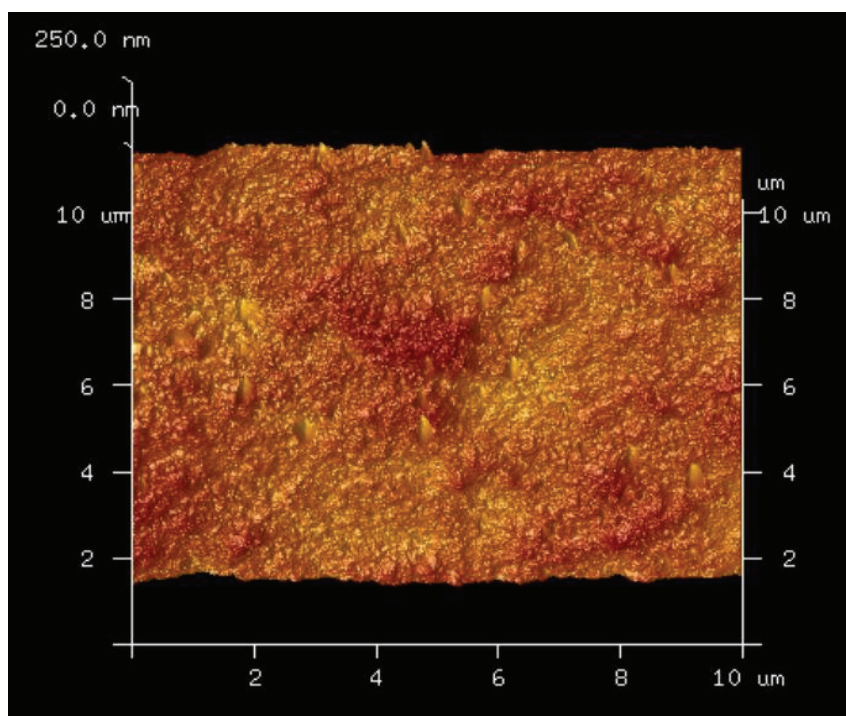


Figure 4.20. AFM images of support membrane (PAI/PEI).

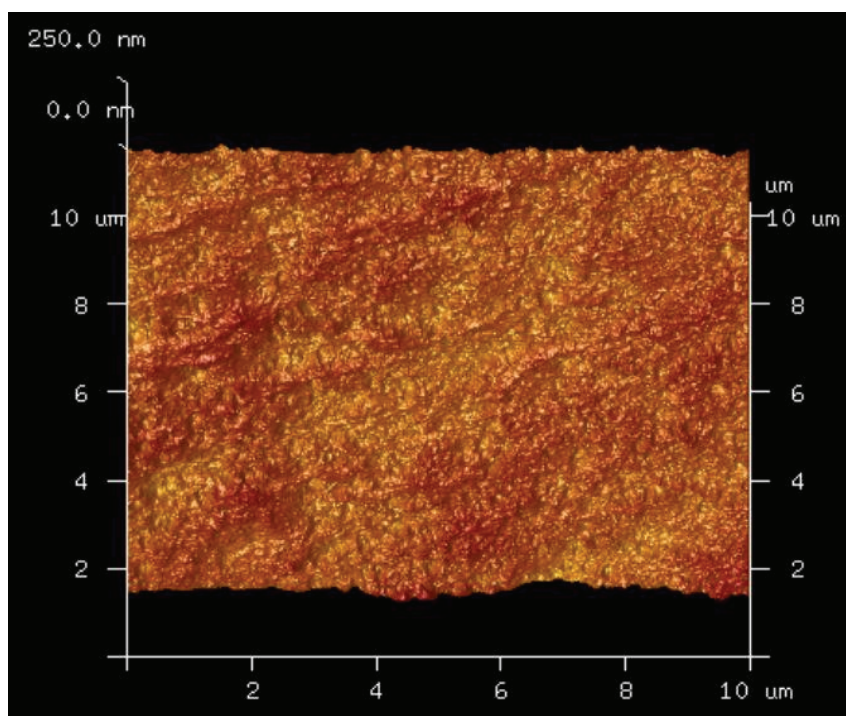


Figure 4.21. AFM images of modified membrane (PAI/PEI_Alginate).

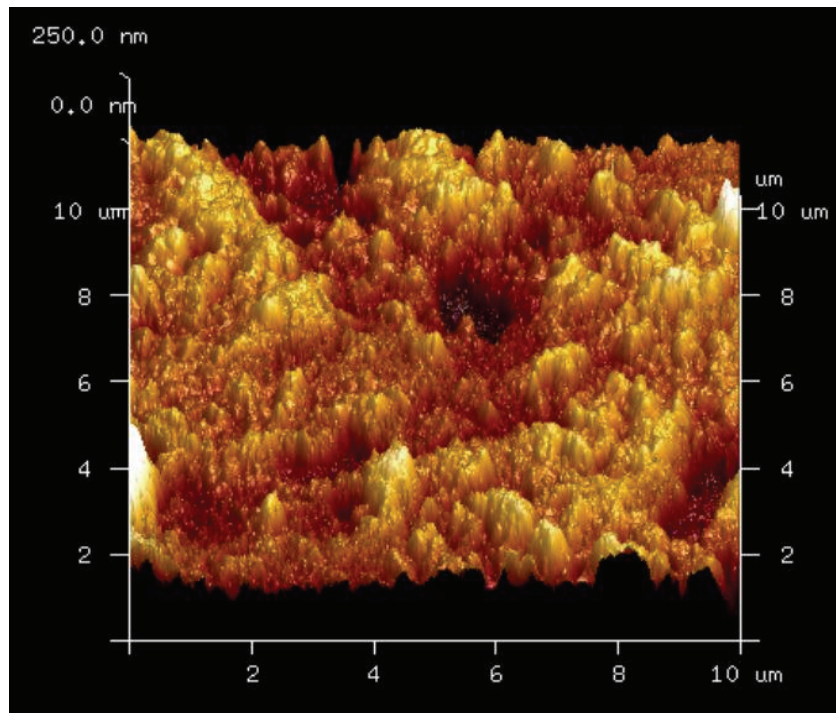


Figure 4.22. AFM images of modified membrane (PAI/PEI/Alginate/Fe³⁺).

Table 4.11. Surface roughness values of bare and modified membranes.

Membranes	Ra (nm)	Rq (nm)
PAI/PEI	8.17	10.3
PAI/PEI_Alginate	6.20	7.70
PAI/PEI/Alginate/Fe⁺³	27.6	36.8

The long-term separation performance of the PAI/PEI/Alginate/Fe³⁺ membrane was first evaluated by filtering a model mixture that contains 100 ppm dye (Methyl Green) and 1000 ppm salt (NaCl) for 72 h at 2 bar. The samples were collected at regular intervals during the filtration. Figure 4.23 indicated that the modified membrane has negligible fluctuations in rejections to the dye and salt over the entire test of 72 h. The rejection of methyl green is almost 95 % and the NaCl rejection is around 11 %. Solute permeability also did not change during the dye/salt filtration and reported as 22.1 L/m² h bar. After 72 hours of filtration, the membrane was washed with DI-water for 1 hour. The pure water permeability of the membrane was re-measured as 24.6 L / m² h bar. Flux

recovery of our membrane after washing with water was determined to be 93.7% (Figure 4.23).

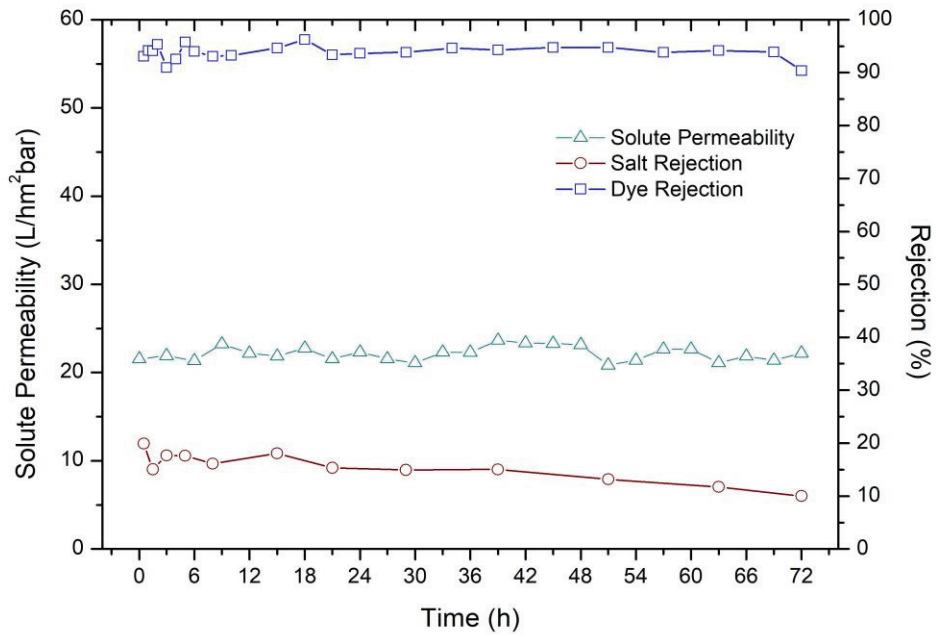


Figure 4.23. Long term separation performance of the membrane toward NaCl and methyl green.

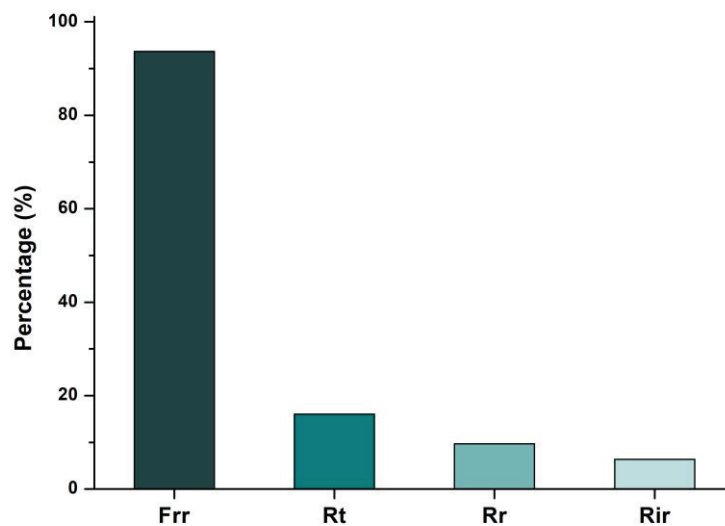


Figure 4.24. Fouling resistances and flux recovery ratio of the modified membrane after filtration of model solution for 72 h.

The dye/salt separation performance of the PAI/PEI/Alginate/Fe³⁺ membrane was compared with those reported in the literature (Table 4.12). It should be noted that the longest filtration (72 h) was carried in this study. In addition, except reactive red 49, all other dyes have larger sizes than the methyl green used in this study. The dye rejection is controlled by a combination of size exclusion and Donnan exclusion. The size exclusion depends on the difference between the size of the dye molecule and size of the surface pores while Donnan exclusion is controlled by the charge density of the membrane. The highest throughput belongs to the TA-PEI/PES membrane for the separation of congo red from NaCl. However, the rejection was measured at the end of 10 hours while the rejections in this study was measured at the end of 3 days. Excluding this relatively short-term study, the throughput of the PAI/PEI/Alginate/Fe³⁺ membrane was found higher than the throughput of the other membranes reported in the literature. The PAI/PEI/Alginate/Fe³⁺ membrane has shown even higher performance than the membranes tested with larger sized dyes.

Table 4.12. Long-Term separation performance of various lab-scale NF membranes for dye desalination (Feed: 1000 ppm NaCl and 100 ppm dye or *500 ppm dye).

Membranes	Feed	MW (Da)	Solute Permeability (L/m ² hbar)	Rdye (%)	Rsalt (%)	Throughput (L/m ² hbar)	Selectivity	Filtration Time (h)	Refs.
LDHs/PEI-M	Methyl blue/NaCl	799.8	8.0	97.9	3.0	7.6	46.2	30	(Zhao et al. 2018)
Fe (III)-phos-(PEI)/HPAN	Methyl blue/NaCl	799.0	5.7	99.8	8.1	5.2	437.7	30	(Li, Wang, et al. 2018)
mHT/PES	*Reactive black 5/NaCl	991.8	4.0	96.0	12.0	3.4	22.0	48	(Yu et al. 2016)
	*Reactive red 49/NaCl	576.5	3.5	91.0	10.0	2.8	10.0	48	
SiO ₂ -PIL/PES	*Reactive black 5/NaCl	991.8	11.5	93.0	6.0	10.0	13.4	48	(Yu et al. 2015)
	*Reactive red 49/NaCl	576.5	13.0	87.0	7.0	10.4	7.2	48	
PAN/PEI	Methyl blue/NaCl	800.0	16.0	97.0	2.0	15.2	32.7	30	(Zhao and Wang 2017)
	Congo red/NaCl	696.0	16.0	97.3	2.0	15.2	36.3	30	
TA-PEI/PES	Congo red/NaCl	696.0	41.5	99.8	8.4	37.93	458	10	(Li et al. 2019)
PAI/PEI_Alg_Fe ³⁺	Methyl green/NaCl	603.0	22.0	95.0	11.3	18.4	17.8	72	In This Work

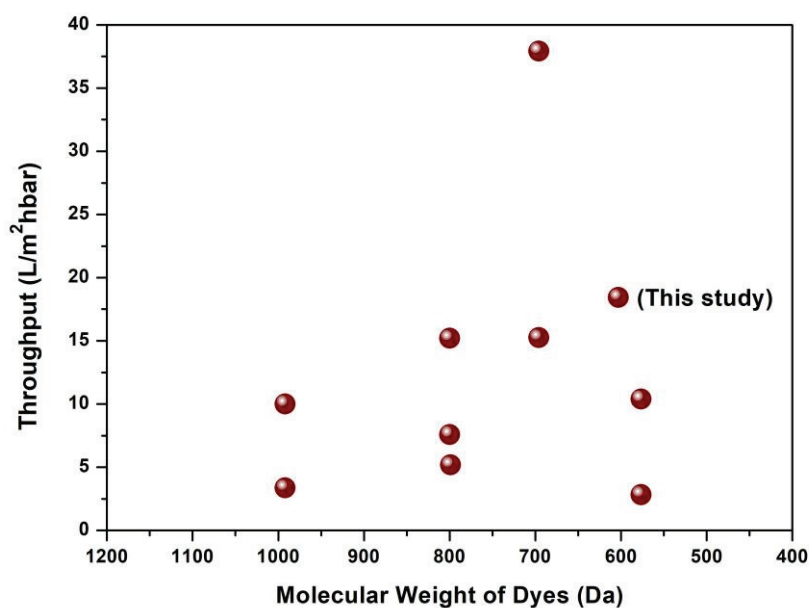


Figure 4.25. Throughput comparison of different membranes from literature.

Most of the newly developed membranes were tested with model one-component or two-component feed streams, whereas the actual textile wastewater contains complex mixtures of multiple components. The interaction of these particular components with one another and with membrane surfaces can cause unpredictable behavior compared to the one-component tests (Bengani-Lutz et al. 2017). Therefore, long-term stability tests were carried out in a cross-flow system for 72 hours with the real textile wastewater samples. The wastewater samples were received from ‘Ekoten Fabrics’ in İzmir, Turkey. The sample was dark blue in color and the COD, TOC, TDS, color, and pH parameters of this sample are given in Table 4.13. The total amount of suspended solids in this textile wastewater sample is higher than the other textile wastewater streams according to Verma et al. (2012). Therefore, the sample was first centrifuged at 7000 rpm for 10 minutes before passing through the membrane. The change in the flux of the wastewater sample as a function of time is shown in Figure 4.26. It was noted that the flux of the wastewater stream ($11.2 \text{ L/m}^2 \text{ h}$) at 2 bar is lower than the flux of the model dye solution (dye + salt solution) ($44.2 \text{ L/m}^2 \text{ h}$) at the same transmembrane pressure. At the end of 72 hours filtration, the flux decreased by 43 %. The decrease in flux occurs due to accumulation on the surface and clogging of the pores by dyes, dye auxiliaries, inorganic salts and surfactants in the wastewater. Tables 4.13 and 4.14 show the

properties of wastewater before and after biological and membrane treatment respectively. The company applies biological treatment to its produced wastewater and as shown in Table 4.13, the treated water satisfies the discharge criteria. Similarly, the wastewater treated with the PAI/PEI_Alq_Fe membrane also satisfied the discharge criteria (Table 4.14). However, the membrane filtration allowed higher color removal and the COD of the water treated with water was found lower compared to the water samples treated biologically in the company's wastewater treatment unit. Figure 4.27 shows the change in the color of the wastewater samples after centrifugation and filtration.

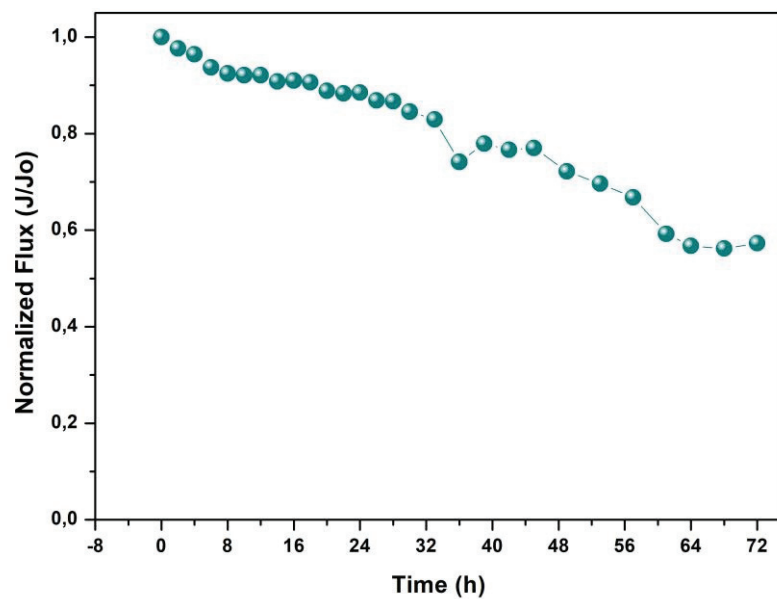


Figure 4.26. Long term separation performance of the resulted membrane toward real textile wastewater.

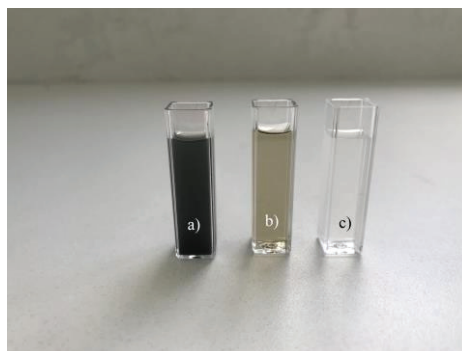


Figure 4.27. (a) Real textile wastewater, (b) After centrifugation of real textile wastewater (feed), and (c) After membrane treatment.

Table 4.13. Real textile wastewater properties.

Parameters	Real Textile Wastewater	After Company Treatment	Discharge Criteria
COD (mg/L)	2075	141	250-400
Color (Pt-Co)	2504	220	260-280
TSS (mg/L)	1253	26	100-400
TOC (mg/L)	489	68	-
TDS (mg/L)	5380	6550	-
Conductivity (mS/cm)	7.66	9.05	-
pH	7.51	7.72	6-9

Table 4.14. Membrane rejection performance in the treatment of real textile wastewater samples.

Parameters	Feed (After Centrifugation of Company Wastewater)	After Membrane Treatment (72h)	Rejection (%)	Discharge Criteria
COD (mg/L)	531	105	80.23	250-400
Color (Pt-Co)	1792	137	92.35	260-280
TSS (mg/L)	240	40	83.33	100-400
TOC (mg/L)	232	80	65.5	-
TDS (mg/L)	4910	4680	4.7	-
Conductivity (mS/cm)	8.25	7.55	8.48	-
pH	7.64	8.02	-	6-9

CHAPTER 5

CONCLUSIONS

In this thesis, a novel positively charged NF membrane was developed for dye and salt separation in textile wastewater. The support membranes of various pore sizes were produced by changing the composition of the coagulation bath and casting solution during the non-solvent phase inversion method. The optimum support membrane exhibiting the highest PWP was in-situ modified with the alginate and coordinated with the Zn^{2+} and Fe^{3+} ions to achieve both high permeability and high selectivity. The membrane was optimized by examining the effects of metal ions concentration and reaction time on the membrane performance. It has been demonstrated that the optimized membrane had high solute permeability ($>22 \text{ L} / \text{m}^2 \text{ h bar}$), high dye rejection ($\sim 95 \%$) and low salt rejection ($\sim 11 \%$) during long-term filtration of model dye and salt solution. Moreover, this membrane was tested in the treatment of real textile wastewater samples generated from a textile dyeing plant in Turkey. The wastewater sample has reached discharge standards after membrane treatment. The membrane showed high color removal ($> 92 \%$) while showing low conductivity removal (8 %). This is desirable for the separation of salt from dye so that dye can be evaluated for reuse in the process. Membrane developed in this study has high performance and superior stability in the separation of dye and salt in textile wastewater treatment.

REFERENCES

- Al-Musa, S., Abu Fara D., and A.A. Badwan. 1999. "Evaluation of parameters involved in preparation and release of drug loaded in crosslinked matrices of alginate." *Journal of Controlled Release* (57):223-232.
- Bengani-Lutz, Prity, Ruken Dilara Zaf, P. Zeynep Culfaz-Emecen, and Ayse Asatekin. 2017. "Extremely fouling resistant zwitterionic copolymer membranes with ~ 1 nm pore size for treating municipal, oily and textile wastewater streams." *Journal of Membrane Science* 543:184-194.
- Cheng, S., D. L. Oatley, P. M. Williams, and C. J. Wright. 2011. "Positively charged nanofiltration membranes: review of current fabrication methods and introduction of a novel approach." *Adv Colloid Interface Sci* 164 (1-2):12-20.
- Choudhury, Rikarani R., Jaydevsinh M. Gohil, Smita Mohanty, and Sanjay K. Nayak. 2018. "Antifouling, fouling release and antimicrobial materials for surface modification of reverse osmosis and nanofiltration membranes." *Journal of Materials Chemistry A* 6 (2):313-333.
- Fan, Lin, Yanyan Ma, Yanlei Su, Runnan Zhang, Yanan Liu, Qi Zhang, and Zhongyi Jiang. 2015. "Green coating by coordination of tannic acid and iron ions for antioxidant nanofiltration membranes." *RSC Advances* 5 (130):107777-107784.
- Geoff Rayner-Canham, Tina Overton. 2014. *Descriptive Inorganic Chemistry*: W. H. Freeman and Company A Macmillan Higher Education Company.
- Guillen, Gregory R., Yinjin Pan, Minghua Li, and Eric M. V. Hoek. 2011. "Preparation and Characterization of Membranes Formed by Nonsolvent Induced Phase Separation: A Review." *Industrial & Engineering Chemistry Research* 50 (7):3798-3817.
- Han, G., T. S. Chung, M. Weber, and C. Maletzko. 2018. "Low-Pressure Nanofiltration Hollow Fiber Membranes for Effective Fractionation of Dyes and Inorganic Salts in Textile Wastewater." *Environ Sci Technol* 52 (6):3676-3684.
- Hermans, Sanne, Hanne Mariën, Cedric Van Goethem, and Ivo F. J. Vankelecom. 2015. "Recent developments in thin film (nano)composite membranes for solvent resistant nanofiltration." *Current Opinion in Chemical Engineering* 8:45-54.
- Ismail, Ahmad Fauzi , and Lau Woei Jye. 2017. *Nanofiltration membranes synthesis, characterization, and applications*: CRC Press.
- Jun, Lau Yien, Lau Sie Yon, N. M. Mubarak, Chua Han Bing, Sharadwata Pan, Michael K. Danquah, E. C. Abdullah, and Mohammad Khalid. 2019. "An overview of

- immobilized enzyme technologies for dye and phenolic removal from wastewater." *Journal of Environmental Chemical Engineering* 7 (2).
- Li, Jie, Xinguo Si, Xiaoqing Li, Naixin Wang, Quanfu An, and Shulan Ji. 2018. "Preparation of acid-resistant PEI/SA composite membranes for the pervaporation dehydration of ethanol at low pH." *Separation and Purification Technology* 192:205-212.
- Li, Ping, Zhan Wang, Libin Yang, Shuang Zhao, Peng Song, and Bushra Khan. 2018. "A novel loose-NF membrane based on the phosphorylation and cross-linking of polyethyleneimine layer on porous PAN UF membranes." *Journal of Membrane Science* 555:56-68.
- Li, Qin, Zhipeng Liao, Xiaofeng Fang, Dapeng Wang, Jia Xie, Xiuyun Sun, Lianjun Wang, and Jiansheng Li. 2019. "Tannic acid-polyethyleneimine crosslinked loose nanofiltration membrane for dye/salt mixture separation." *Journal of Membrane Science* 584:324-332.
- Mulder, Marcel. 1997. *Basic Principles of Membrane Technology*. 2nd ed. Netherlands: Kluwer Academic Publishers
- Ong, Yee Kang, Fu Yun Li, Shi-Peng Sun, Bai-Wang Zhao, Can-Zeng Liang, and Tai-Shung Chung. 2014. "Nanofiltration hollow fiber membranes for textile wastewater treatment: Lab-scale and pilot-scale studies." *Chemical Engineering Science* 114:51-57.
- Peydayesh, Mohammad, Toraj Mohammadi, and Omid Bakhtiari. 2018. "Effective treatment of dye wastewater via positively charged TETA-MWCNT/PES hybrid nanofiltration membranes." *Separation and Purification Technology* 194:488-502.
- Porter, Mark C. 1991. *Handbook of Industrial Membrane Technology*: Noyes Publication.
- Priyadarshini, Antara, Siok Wei Tay, Pin Jin Ong, and Liang Hong. 2018. "Zeolite Y-carbonaceous composite membrane with a pseudo solid foam structure assessed by nanofiltration of aqueous dye solutions." *Journal of Membrane Science* 567:146-156.
- Ruey-Shin, Juang, and Chen Ming-Nan. 1996. "Measurement of Binding Constants of Poly(ethylenimine) with Metal Ions and Metal Chelates in Aqueous Media by Ultrafiltration." *Ind. Eng. Chem. Res* 35 (6):1935-1943.
- Saburo, Nonogaki, Makishima Shoji, and Yoneda Yukio. 1957. "Polyvalent Anion-exchange resins composed of cross-linked polyethylenimine complexes of heavy metals " *Polyvalent Anion-exchange Resins* 62:601-603.
- Schwab, Klaus. 2016. *The Global Risks Report 2016*. Switzerland: World Economic Forum.

- Soyekwo, Faizal, Qiugen Zhang, Runsheng Gao, Yan Qu, Ruixue Lv, Mengmeng Chen, Aimei Zhu, and Qinglin Liu. 2017. "Metal in situ surface functionalization of polymer-grafted-carbon nanotube composite membranes for fast efficient nanofiltration." *Journal of Materials Chemistry A* 5 (2):583-592.
- Sun, Shi Peng, T. Alan Hatton, Sui Yung Chan, and Tai-Shung Chung. 2012. "Novel thin-film composite nanofiltration hollow fiber membranes with double repulsion for effective removal of emerging organic matters from water." *Journal of Membrane Science* 401-402:152-162.
- Tu, Nguyen Phuong. 2013. "Role of charge effects during membrane filtration." Master Thesis, Faculty of Bioscience Engineering Ghent University.
- Van der Bruggen, B., Schaep J., Maes W., Wilms D., and Vandecasteele C. 1998. "Nanofiltration as a treatment method for the removal of pesticides from ground waters." *Desalination* 117:139-147.
- Verma, A. K., R. R. Dash, and P. Bhunia. 2012. "A review on chemical coagulation/flocculation technologies for removal of colour from textile wastewaters." *J Environ Manage* 93 (1):154-68.
- Xu, Jia, Lili Zhang, Xueli Gao, Haiyan Bie, Yunpeng Fu, and Congjie Gao. 2015. "Constructing antimicrobial membrane surfaces with polycation-copper(II) complex assembly for efficient seawater softening treatment." *Journal of Membrane Science* 491:28-36.
- Xu, Yan Chao, Zhen Xing Wang, Xi Quan Cheng, You Chang Xiao, and Lu Shao. 2016. "Positively charged nanofiltration membranes via economically mussel-substance-simulated co-deposition for textile wastewater treatment." *Chemical Engineering Journal* 303:555-564.
- Yang, Libin, Zhan Wang, and Jinglong Zhang. 2017. "Zeolite imidazolate framework hybrid nanofiltration (NF) membranes with enhanced permselectivity for dye removal." *Journal of Membrane Science* 532:76-86.
- Yu, L., Y. Zhang, Y. Wang, H. Zhang, and J. Liu. 2015. "High flux, positively charged loose nanofiltration membrane by blending with poly (ionic liquid) brushes grafted silica spheres." *J Hazard Mater* 287:373-83.
- Yu, Liang, Jianmian Deng, Huixian Wang, Jindun Liu, and Yatao Zhang. 2016. "Improved Salts Transportation of a Positively Charged Loose Nanofiltration Membrane by Introduction of Poly(ionic liquid) Functionalized Hydrotalcite Nanosheets." *ACS Sustainable Chemistry & Engineering* 4 (6):3292-3304.
- Zhao, Shuang, and Zhan Wang. 2017. "A loose nano-filtration membrane prepared by coating HPAN UF membrane with modified PEI for dye reuse and desalination." *Journal of Membrane Science* 524:214-224.
- Zhao, Shuang, Hongtai Zhu, Zhan Wang, Peng Song, Min Ban, and Xufeng Song. 2018. "A loose hybrid nanofiltration membrane fabricated via chelating-assisted in-situ

growth of Co/Ni LDHs for dye wastewater treatment." *Chemical Engineering Journal* 353:460-471.